An improved workflow for image- and laser-based virtual geological outcrop modelling

ALEKSANDRA A. SIMA

Dissertation for the degree philosophiae doctor (PhD)
at the University of Bergen

2013

Dissertation date: 15 March 2013

Scientific environment

The research presented in this thesis has been conducted at the Centre for Integrated Petroleum Research (Uni CIPR) in Bergen, Norway as a part of the Empirical Understanding of Sedimentary Architecture (EUSA) project, a Petromaks project funded by the Research Council of Norway and FORCE (grant 193059). During this research I have also been enrolled in the PhD studies at the Department of Informatics, University of Bergen. Furthermore, parts of the research were carried out in collaboration with Technische Universität Dresden, Germany as well as with the Institut d'Informàtica i Aplicacions, Universitat de Girona, Spain, which I visited as a guest researcher.

Acknowledgements

First and foremost my sincere gratitude goes to my supervisor, Simon Buckley, who provided guidance, support and encouragement throughout the course of this research. He always found time for discussions and numerous revisions of our manuscripts. I would also like to thank him for his understanding of my relocation during this research and trust in my self-discipline to work from home.

Ivan Viola is thanked for fruitful brainstorming, enthusiasm and guidance in the domain of visualisation. I am grateful to Danilo Schneider for being a connection to the photogrammetric world, sharing knowledge and all the support with the Bundle software. I would also like to thank to John Howell for intriguing discussions and spreading around his passions for geology and life in general. Thanks also go to Xavier Bonaventura, Miquel Feixas and Mateu Sbert for an excellent introduction to the basics of information theory and showing me the best of Girona.

Andreas and Steffi Rittersbacher are thanked for the relaxing time that we spent together, the never-ending support and willingness to talk, laugh and enjoy life. Tobias Kurz is thanked for nice talks, encouragement and sharing his experiences, not only in hyperspectral data processing, but also in survival. Thanks also go to Christian Haug Eide, Oliver Severin Tynes, Björn Nyberg, Kim Senger, Nicole Naumann and Luisa Zuluaga for joyful lunches and coffee breaks. I am not forgetting all the colleagues at Uni CIPR who created a pleasant and positive working environment.

This work would not have been possible without funding from the Norwegian Research Council, the Centre for Integrated Petroleum Research (Uni CIPR) and the FORCE consortium. Several travels were financed by Statoil ASA, through the Akademia agreement. NAGRA, Swisstopo and the Mont Terri Consortium are thanked for support in data collection. Riegl GmbH is acknowledged for providing software support.

I wish to express my most heartfelt gratitude and appreciation to my parents and my brother for their love and encouragement throughout my life. Finally, I would like to especially thank my love, Rafal, for all the warmth that he gives me.

Abstract

Photorealistic 3D models, representing an object's surface geometry textured with conventional photography, are used for visualization, interpretation and spatial measurement in many disparate fields, such as cultural heritage, archaeology and throughout the earth sciences, including geology. Virtual models of geological outcrops allow for large quantities of geometric data, such as sizes of features, thicknesses of strata, or surface orientations to be extracted in relatively short time and in areas with difficult accessibility. However, standard analysis is limited to interpretation of the three standard spectral bands (red, green, blue; RGB) acquired in the visible spectrum by the conventional digital camera. Complementing the photorealistic 3D outcrop models with auxiliary spectral data, for example in the form of hyperspectral imagery, can provide domain experts with additional geochemical information, adding great potential to studies of mineralogy and lithology.

The existing workflows for creation of photorealistic outcrop models and integration with terrestrial panoramic hyperspectral data are complex and require specific knowledge from the field of geomatics. One such processing step is selection of images taking part in the texture mapping process. Although automated texture mapping measures are available, in highly redundant image sets they do not necessarily provide the best results when using all available photos. Therefore selection of the most suitable texture candidates is required to increase the realism of the textured models and the processing efficiency. Especially for large models of rugged terrain, represented by millions of triangles, manual selection of the best texture candidates can be challenging, because the user must account for occlusions and ensure that image overlap is sufficient to cover relevant model triangles.

The existing workflow for integration of hyperspectral and 3D data also requires specific skills in geomatics as homologous points between the two datasets need to be manually selected for registration. Finding such correspondences involves interpretation of data acquired with different sensors, in different parts of the electromagnetic spectrum, projections and resolutions. The need to complete such

challenging data processing steps by users from outside the geomatics domain poses a serious obstacle to these methods becoming standardised across geological research and industry.

The research presented in this thesis addressed the two aforementioned limitations in the data processing workflows with an aim to make the method more accessible for users from outside of the geomatics domain. Firstly, a new interactive framework was developed, that provides analytical and graphical assistance in selection of an image subset for geometrically optimised texturing in photorealistic 3D models. Visualisation of spatial relationships between different components of the datasets was used to support the user's decision in tasks requiring specific technical background. Novel texture quality measures were proposed and new automatic image sorting procedures, originating in computer vision and information theory, were implemented and tested. The image subsets provided by the automatic procedures were compared to manually selected sets and their suitability for 3D model texturing was assessed. Results indicated that the automatic sorting algorithms can be a valid alternative to manual methods. The resulting textured models were of comparable quality and completeness, and the time spent in time-consuming reprocessing was reduced. Anecdotal evidence indicated an increased user confidence in the final textured model quality and completeness.

Secondly, a method for semi-automatic registration of terrestrial hyperspectral imagery with laser and image data was developed. The proposed data integration procedure employed the Scale Invariant Feature Transform (SIFT) to automatically find homologous points between digital RGB images registered in the scanner coordinate system and short wave infrared cylindrical hyperspectral data. The need for large numbers of homologous points to be matched required optimisation of the SIFT operator, as well as a routine for eliminating false matches. The proposed method automatically provides the control points that are used for registering the hyperspectral imagery. The results obtained on two datasets with different characteristics indicated that the proposed method can be used as an alternative to manual data integration, saving time and minimizing user input during processing.

The increased automation of the workflows for creation of photorealistic outcrop models and integration with auxiliary image data, complemented with computer assistance to support users' decision in the processing steps requiring background in geomatics, facilitate adoption of such techniques in wider community.

Related Publications

This thesis is based on the following peer reviewed publications:

(A) **A. A. Sima**, S. J. Buckley, I. Viola, 2012. An interactive tool for analysis and optimization of texture parameters in photorealistic virtual 3D models. *ISPRS Annals of the Photogrammetry, Remote Sensing and Spatial Information Sciences,* I-2: 165-170.

(B) **A. A. Sima**, X. Bonaventura, M. Feixas, M. Sbert, J. A. Howell, I. Viola, S. J. Buckley, in press. Computer-aided image geometry analysis and subset selection for optimizing texture quality in photorealistic models. *Computers & Geosciences*, Elsevier, http://dx.doi.org/10.1016/j.cageo.2012.11.004

(C) **A. A. Sima**, S. J. Buckley, T. H. Kurz, D. Schneider, 2012. Semi-automatic integration of panoramic hyperspectral imagery with photorealistic lidar models. *Photogrammetrie, Fernerkundung, Geoinformation (PFG) 2012 / 4: 439–450.*

(D) **A. A. Sima**, S. J. Buckley, T. H. Kurz, D. Schneider. Semi-automated registration of close range hyperspectral images using terrestrial lidar and image datasets. Submitted to *The Photogrammetric Record*.

(E) **A. A. Sima**, S. J. Buckley. Optimizing SIFT for matching short-wave-infrared and visible images. Submitted to *Remote Sensing*.

All the listed manuscripts were written during the PhD research by the author of this thesis with the support of Simon Buckley, who contributed with project guidance and assistance during manuscript revision. Paper A and Paper B are co-authored by Ivan Viola, who helped to mature the ideas developed during numerous discussions, as well as helping navigate through the visualisation domain. Paper B is also co-authored by Xavier Bonaventura, Miquel Feixas and Mateu Sbert, who made the principles of Information Theory understandable and contributed with their knowledge and experience in development of the information-driven image sorting algorithms. John Howell provided general project mentoring and helped to bring

inspiration from the user domain. Paper C and Paper D are co-authored by Tobias Kurz who, in addition to collection of the hyperspectral data, contributed to a better understanding of the nature of hyperspectral imaging and the HySpex SWIR-320m camera in numerous discussions. Danilo Schneider contributed with photogrammetric and statistical knowledge and made his software, Bundle, available for the purposes of this research.

The following publications are also related to but not included in this thesis:

A. A. Sima, S. J. Buckley, D. Schneider, J. A. Howell, 2010. An improved workflow for image- and laser-based virtual geological outcrop modelling. *Proceedings of PCV 2010 - Photogrammetric Computer Vision and Image Analysis, 1–3 September 2010, Saint-Mandé, France. International Archives of the Photogrammetry, Remote Sensing and Spatial Information Science, XXXVIII, part 3: 115-120.*

T. H. Kurz, S. J. Buckley, D. Schneider, **A. A. Sima** and J. A. Howell, 2011. Ground-based hyperspectral and lidar scanning: a complementary method for geoscience research. *Proceedings of the International Association of Mathematical Geosciences Conference, 5-9th September, Salzburg, Austria, 1441-1451.*

Contents

Part I

Overview

Chapter 1

Introduction

With recent hardware developments and increased software automation, the range of applications of photorealistic 3D models of real-world scenes has diversified rapidly. These models, geometrically representing the object surface and textured with conventional photography are used in heritage documentation (Portales at al. 2009; Duca et al. 2011), virtual tourism (Remondino 2011) and archaeology (Wulff 2010), as well as in urban planning (Bénitez and Baillard 2009), mining (González-Aguilera et al. 2012), and the earth sciences, such as in landslide modelling (Niethammer et al. 2012) or geology (Buckley et al. 2008a; Sturzenegger and Stead 2009; Fabuel-Perez et al. 2009; Rittersbacher et al. 2012).

3D modelling of geological outcrops, such as exposed cliff sections or quarries, can be used to improve understanding of subsurface geology. Photorealistic outcrop models (Figure 1.1) allow for interpretation and measurements of geological features, i.e. sizes of objects, thicknesses of strata or surface orientation, that can be used for populating stochastic models of subsurface reservoirs, for example in the oil and gas industry (Bellian 2005; Pringle et al. 2006; Enge et al. 2007; Buckley et al. 2008a; Jones et al. 2009; Fabuel-Perez et al. 2009; Rittersbacher et al. 2012). The geological interpretation can be performed on the screen, also in inaccessible areas where conventional fieldwork methods may be unsafe. The virtual outcrop measurement methods allow not only for large quantity of data to be collected in relatively short time, but also provide support to improve documentation of field observations (Bellian 2005).

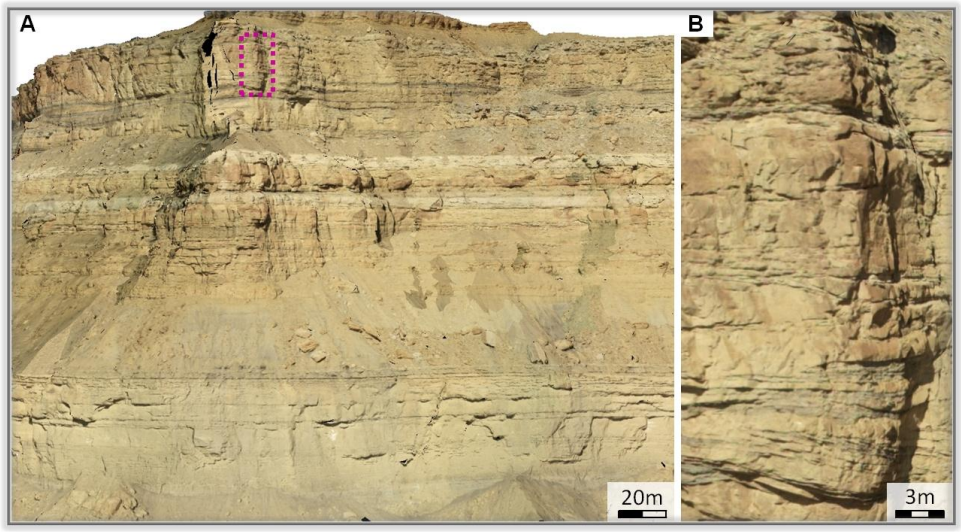

Figure 1.1. (A) Photorealistic 3D outcrop model covering a section of the Book Cliffs, Utah, USA. Model area marked in purple enlarged in (B).

Though the 3D photorealistic models themselves are a valuable source of information, greater benefit can be gained by complementing them with data acquired by other sensors. In recent years, a number of sophisticated imaging devices, customised for specific needs, have been developed and subsequently adopted by the remote sensing community, providing new opportunities for interdisciplinary studies. In photorealistic outcrop models mineralogical and lithological mapping is normally limited to interpretation of the data recorded in three standard spectral bands (red, green, blue; RGB) of the visible spectrum. Many minerals exist that cannot be distinguished using visible light, but that exhibit specific absorption and reflectance properties in the infrared region of the electromagnetic spectrum, e.g. limestone and dolomite (van der Meer and de Jong 2001). Therefore, complementing the virtual outcrop models with auxiliary spectral data, i.e. short wave infrared (SWIR) hyperspectral imagery (Figure 1.2), can provide additional geochemical information and help to understand information invisible to the naked eye, adding great potential to studies of mineralogy and lithology (Kurz et al. 2012).

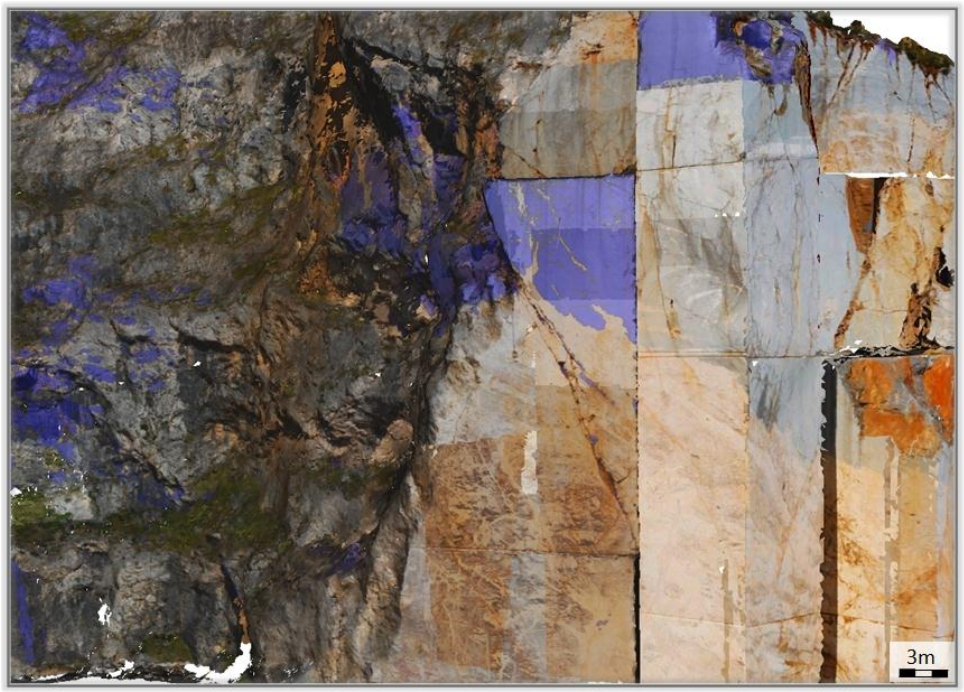

Figure 1.2. 3D outcrop model textured with RGB images and results of hyperspectral classification. Limestone patches marked in blue.

The workflow for collecting and using virtual outcrop data has been developed and applied in reservoir modelling in recent years (Bellian 2005; Enge et al. 2007; Buckley et al. 2008a; Buckley et al. 2008b). An approach to complement the 3D textured models with data acquired by a portable terrestrial SWIR hyperspectral sensor has also been established and proved (Kurz et al. 2011; Kurz et al. 2012). Although both methods have been successfully used, they represent a complex sequence of processing steps that often require time-consuming manual work and specific technical background, significantly impeding the prevalence of textured 3D models outside of the geomatics domain.

Therefore, before such methods are standardised across geological research and industry, further research is required to improve and automate processing steps where most technical background and skills in geomatics are required.

1.1 Research scope

The aim of this thesis is to make the existing workflow for creation of photorealistic outcrop models more accessible for users from outside of the geomatics domain, specifically by increasing the level of automation in processing and providing decision support in tasks requiring most technical background or experience. Two areas of the workflow (Figure 1.3), identified as bottlenecks for processing and reflecting a very practical need on the behalf of the users, are targeted. A by-product of the workflow improvements is to decrease the overall data processing time.

1.2 Structure of the thesis

This thesis comprises two complementary parts. The first part aims to give a broad background to the thesis' contribution and starts with an overview of the existing workflow for creation of photorealistic 3D outcrop models (Chapter 2). Research related to integration of 3D models with ancillary image data (Chapter 3) is assessed, and followed by a summary of individual contributions of the thesis (Chapter 4). Conclusions and potential future work are presented in Chapter 5. The second part or the thesis consists of five publications, provided as they were published or submitted to the journals, with only minor adjustments in formatting to fit the format of this dissertation.

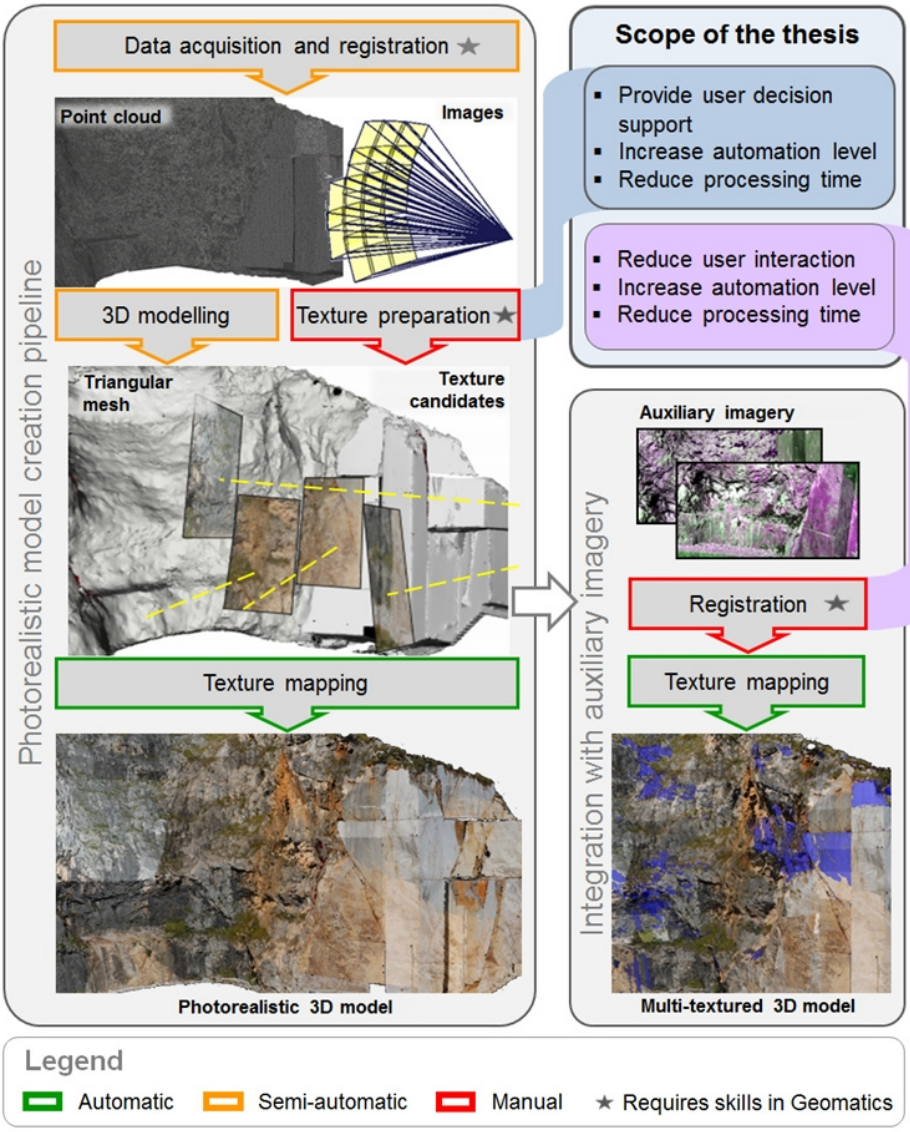

Figure 1.3. General workflow for creation of photorealistic 3D models and integration with auxiliary image data, with a highlight of the two areas addressed in this thesis.

Chapter 2

Creation of photorealistic 3D outcrop models: Background

Developments in the workflow for creation of photorealistic 3D models (Debevec and Taylor 1996) of geological outcrops are documented by several authors (Bellian 2005; Pringle et al. 2006; Buckley et al. 2008a; Buckley et al. 2008b). Although depending on the object size and accuracy requirements, different approaches to data acquisition and registration can be applied with similar processing results, i.e. the 3D terrain geometry is reconstructed and combined with digital images to provide the photorealistic effect.

The workflow for creation of virtual outcrop models presented in this section is a summary of methods presented in Buckley et al. 2008a and Buckley et al. 2008b, complemented with alternative solutions reported in literature, as well as an outline of image-based modelling techniques to provide a broader overview of different data acquisition and processing approaches. However, because the datasets used in this research were acquired using laser scanning, laser-based techniques are presented in greater detail.

The workflow presented in Figure 2.1 is an extended version of the sketch shown in Figure 1.3 (left), complemented with indicators of the level of automation and approximate amount of time required to accomplish each processing stage. The processes that require most knowledge or skills in geomatics are also marked.

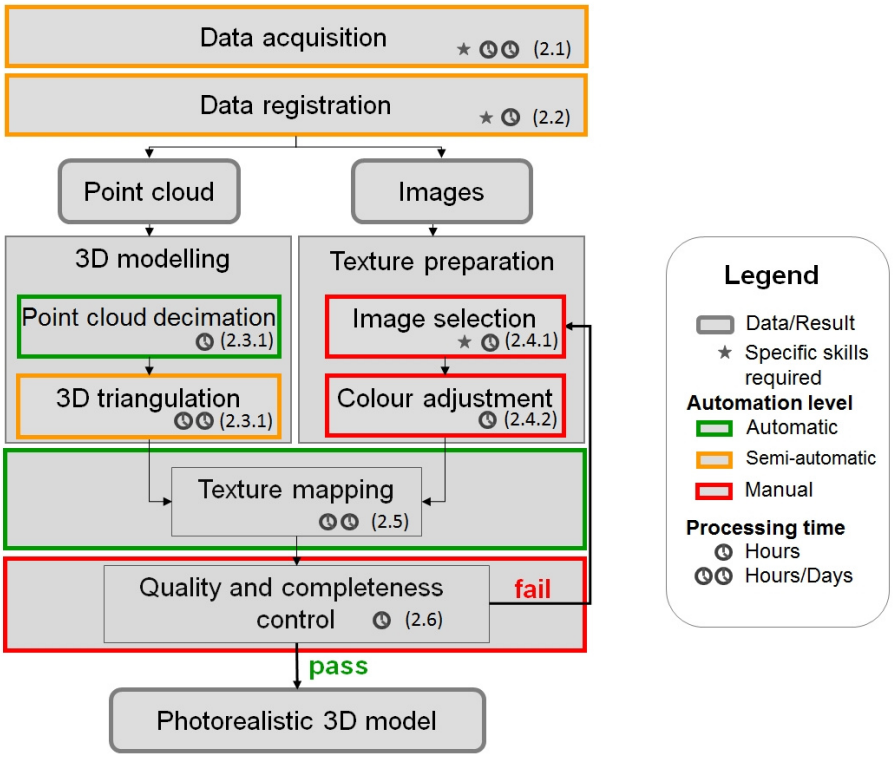

Figure 2.1. Workflow for creation of textured photorealistic 3D models (modified after Buckley et al. (2008a)).

Creation of photorealistic 3D models of real word scenes requires two types of information being available: 3D geometry of the object surface and imagery covering the scene allowing for realistic texture generation. The surface of complex scenes can be reconstructed using laser scanning, photogrammetric methods or a combination of the two (Remondino 2006). The choice of the surface modelling technique depends on the size, accessibility and characteristics of the object. Therefore prior to data acquisition the purpose of the study and the arising requirements for the virtual models need to be analysed.

2.1 Data acquisition

For models of large, complex and irregular surfaces, where high resolution and high accuracy are essential, 3D data is commonly acquired (El-Hakim et al. 2008) using laser scanners (LIght Detection and Ranging - LIDAR) that are active sensors directly

capturing the 3D object geometry based on range measurements. Although the laser scanning measurements can be based on: time-of-flight, phase shift or triangulation, the first technology dominates the topographic survey market (Buckley et al. 2008a; Remondino 2011). In the time-of-flight based scanners the range is determined based on the measured return time of an emitted laser pulse (Vosselman and Maas 2010). The coverage of the pre-selected scanner field of view is realised by deflection of the laser beam over a calibrated angular grid with point spacing defined by the operator. The 3D object coordinates are computed using horizontal and vertical laser pulse deflection angles combined with the range. Modern laser scanners are capable of measuring hundreds thousands of points per second and recording additional information, i.e. intensity of the reflected laser signal.

Terrestrial laser scanners can acquire data from a distance of a few centimetres to a few kilometres (Remondino 2011). Depending on the size and scale of the study, an instrument with suitable characteristics should be chosen. The trade-off is between the range, accuracy, beam diameter, optical wavelength and the cost of the scanner (Luhmann et al. 2007). In the case of terrestrial laser scanning (TLS) for geological applications, where the objects can be several hundred meters in extent, a common solution is to use a medium- or long-range (respectively 25m - 250m and > 250m (Lemmens 2007)) scanners rigidly coupled with a calibrated digital single lens reflex (SLR) camera (Buckley et al. 2008a, Heritage and Large 2009).

2.1.1 Terrestrial laser scanning and image acquisition

Although laser scanners are capable of rapid measurements covering large areas with high point density, data acquisition from multiple locations is normally required, not only because of the outcrop size, but due to data shadows or occlusions from vegetation and other unwanted objects. In such cases the adjacent scans should be acquired with overlap greater than 10% of the area (Bellian 2005) in order to ensure sufficient prerequisites for the relative scan registration. To provide the most accurate and realistic virtual outcrop model, the data should be captured perpendicular to the outcrop wall (Bellian 2005; Buckley et al. 2008b; Soudarissanane et al. 2011).

Depending on the characteristics and accessibility of the scanned outcrop section, appropriate lenses should be mounted on the SLR camera attached to the scanner. The camera lenses should be periodically calibrated and the focal lengths fixed for the duration of the data collection. In order to ensure optimal texture mapping conditions, and therefore high realism of the photorealistic look, the photos should be collected so that the image rays are as close to normal to the outcrop face as possible (Debevec and Taylor 1996). Because the scanner position might not be optimal for such image acquisition, e.g. far away from the outcrop face or too oblique, or the lighting conditions might be unfavourable, additional freehand photos can be also acquired from different locations or at different time than when the laser data is collected (El-Hakim et al. 2008). After registration (Section 2.2) they can be used in the texture mapping process (Section 2.5) to create integrated products (El-Hakim et al. 2004).

In order to register the acquired dataset into a geodetic coordinate system the scanner positions are recorded, e.g. using Global Navigation Satellite System (GNSS) observations post-processed relative to a nearby base station (Bellian 2005; Buckley et al. 2008a).

Although using ground-based data collection has many advantages, it becomes time-inefficient for larger areas and may be unsuitable for modelling of high and extensive cliff sections. Increased scanner tilt angles result in larger 3D model discontinuities caused by scanning shadows (Soudarissanane et al. 2011) and very oblique imagery, both leading to poor quality of the textured model (Buckley et al. 2008b). These limitations can be overcome when acquiring data from a helicopter platform.

2.1.2 Helicopter-based laser scanning and image acquisition

Acquisition of oblique aerial images fills the gap between data provided by nadir looking aerial and terrestrial sensors (Smith et al. 2009). The capability of the helicopter to fly along the outcrop slope provides an opportunity to provide geometrically optimized datasets, captured perpendicularly to the outcrop (Bellian 2005; Buckley et al. 2008b; Soudarissanane et al. 2011). An example of a helicopter-

based hand-held laser scanning and image acquisition for geological applications is reported in Buckley et al. (2008b). The employed Helimap system (Vallet and Skaloud 2004), consisted (the system has been upgraded in the meantime) of a Riegl LMS Q240i-60 airborne laser scanner and a Hasselblad H1 camera, and collected the data with a rate computed as a function of desired point density and flight parameters, up to 10,000 points per second, with a quoted accuracy of 0.02m (one sigma) at 50m range (Riegl 2010). The 22 megapixel Hasselblad H1 camera equipped with a calibrated 35mm lens provided visible-spectrum (RGB) images (Skaloud et al. 2002). For outcrop modelling purposes images are usually collected with 60%-70% forward overlap to allow for complementary stereo-plotting and, if multiple image strips are required, with a degree of sidelap between the strips. The camera and the scanner are rigidly coupled and their position is constantly logged by the GNSS receiver and the inertial navigation system (INS) recording the velocity and orientation of the platform. These observations are supplied to recreate the point cloud and camera orientation parameters. The mapping accuracy of the data delivered by the Helimap system with H1 camera was determined as <0.15m (Vallet 2007).

Despite all the advantages of laser scanning, i.e. high data resolution and accuracy plus the high speed of data acquisition (Golparvar-fard et al. 2011), the technique is relatively expensive. Photogrammetric reconstruction of topography from multiple images taken from convergent views (Remondino and El-Hakim 2006), also referred to as image-based modelling, is regarded as an attractive low-cost approach in 3D model creation (Aguilera and Lahoz 2006; Nex and Rinaudo 2008; Golparvar-fard et al. 2011).

2.1.3 Image-based modelling

Photogrammetry is a part of geomatics that allows for reconstruction of position, orientation, shape and size of objects from images (Kraus 2004). In photogrammetric modelling, the perspective camera model or projective geometry (Pollefeys et al. 2004) is applied to 2D measurements of corresponding features on two or more images to recover 3D object position (Remondino 2006). Other techniques of shape reconstruction are available, e.g. shape from shading (Horn and Brooks 1989) or

shape from 2D edge gradients (Winkelbach and Wahl 2001), but these are not applicable for reconstruction of complex real world scenes.

In the image-based large sets of images are collected using consumer grade or SLR cameras (Remondino et al. 2011). Careful image network design and camera choice is required because both factors, together with the quality of the established camera model, influence the accuracy of the reconstructed surface model (Remondino and El-Hakim 2006). If dataset georeferencing is required, the position of several ground control points, clearly distinguishable in images should also be measured in a geodetic coordinate system, for example using GNSS with data post-processing.

A photogrammetric surface reconstruction requires two fundamental inputs: camera calibration and image orientation. For applications requiring high accuracy results they can be derived separately (Remondino and Fraser 2006). Otherwise they are computed at the same time by solving a self-calibrating bundle adjustment (Remondino et al. 2011), based on coordinates of the corresponding points between the images in a block (tie points). Tie points can be extracted using manual measurements or automated approaches (Remondino and Ressl 2006).

Once the image exterior orientation and camera calibration parameters are known, the surface model can be reconstructed using automatic dense image matching techniques (e.g. Remondino et al. 2008) or interactive feature extraction methods (Remondino and El-Hakim 2006). The resulting point cloud can be complemented with automatically extracted linear features (e.g.: Schmid and Zisserman 2000; Remondino and Zhang 2006) preventing smoothing of edges and therefore crucial for such applications as city modelling.

The most recent multi-image matching approaches are reported in Remondino and Zhang (2006), Hiep et al. (2009), Zhu (2010), (Furukawa and Ponce 2010) and (Pierrot-Deseilligny and Clery 2011). A better insight into general image-based modelling of real world scenes can be found in (Remondino and El-Hakim 2006; Remondino et al. 2008; Barazzetti et al. 2010; Remondino 2011).

Because photogrammetric modelling is mostly suitable for smaller sites (El-Hakim et al. 2008), so far it has been rarely applied in geological applications

(Schober and Exner 2011). With the rapid developments of unmanned aerial vehicles (UAVs) allowing for image acquisition from the air and therefore modelling of larger objects (Remondino et al. 2011), image-based modelling methods become prevalent in an increasing number of applications, including close-range mapping in difficult conditions (Lucieere et al. 2011), heritage documentation (Püschelet al. 2008), archaeology (Eisenbeiss and Sauerbier 2011), mining (González-Aguilera et al. 2012) and agriculture (Dandois and Ellis 2010; Turner et al. 2011; Remondino et al. 2011). A review of image-based modelling solutions for data acquired using UAVs can be found in (Remondino et al. 2011).

Many applications can benefit from combination of laser scanning with photogrammetric modelling. One such example is modelling of large architectural objects (e.g. buildings), that require laser scanning from multiple positions and result in huge number of points representing flat surfaces, but can be relatively quickly modelled using photogrammetric techniques (El-Hakim et al. 2004b). Laser based techniques are preferred for modelling of irregular surfaces, such as sculptures and building ornaments (El-Hakim et al. 2004b).

2.2 Data registration

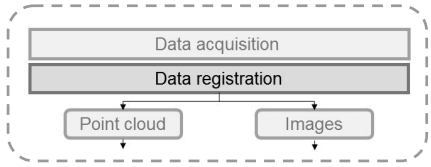

Data acquired with different sensors and/or from multiple positions need to be transformed so that the entire object is represented by a single point cloud and the orientation parameters of collected images are established. Due to the fact that in the image-based modelling the relative image orientation is a part of the 3D surface geometry reconstruction (Section 2.1.3) this processing step is especially valid for the laser-based methods of terrain reconstruction.

2.2.1 Terrestrial laser scanning

In the ground-based datasets all the scans need to be registered into a single coordinate system. This is realised by retrieving a spatial rotation, translation and

scaling of each scan with respect to the reference scan, e.g. a single scan held fixed in the centre of each cliff section (Buckley et al. 2010a). Commonly (El-Hakim et al. 2004a; Bellian 2005; Buckley et al. 2010a) a preliminary manual rough scan alignment is followed by an automatic orientation adjustment using surface matching techniques, i.e. the iterative closest point algorithm (Besl and McKay 1992) or its modifications (e.g. Zhang 1994). Resulting transformation matrices enable the creation of a single point cloud of all the scans. The first, manual step of scan aligning can be performed already during the data acquisition to ensure sufficient scan coverage before moving to the next scanning location (El-Hakim et al. 2008b).

Artificial targets are also used to align multiple scans. Position of the targets can be automatically found in the point cloud directly, on the basis of their geometric (Artese et al. 2004) or geometric and radiometric (Akca 2003) characteristic, or indirectly i.e. using images acquired by a calibrated digital camera rigidly attached to the laser scanner (Al-Manasir and Fraser 2006). For large outcrops the use of control points can be impractical and expensive in field time (Buckley et al. 2010b).

Other techniques, mostly applied for scientific testing only (Alba et al. 2011), allow for pair-wise registration of multiple scans based on homologous points automatically found between intensity data (e.g.: Böhm and Becker 2006; Z. Wang and Brenner 2008) recorded by the scanner or digital images acquired by the camera coupled with the scanner (Al-Manasir and Fraser 2006; Barnea and Filin 2007; González-Aguilera et al. 2009; Alba et al. 2011; Weinmann and Jutzi 2011). The resulting set of matches is used to derive the roto-translation matrices used for the pair-wise scan registration.

Once all the scans are registered into one coordinate system, the project (local) coordinates can easily be transformed to a geodetic coordinate system using the scanner positions derived from the post-processed GNSS observations.

Because the orientation of the camera mounted on the laser scanner is calibrated relative to the scanner centre, the imagery can be registered in the project coordinate system and further used as a texture source in the photorealistic virtual model.

If additional freehand photos were collected, their orientation with respect to the point cloud needs to be established, i.e. they need to be registered in the project

coordinate system. In the processing workflow used in this research, this is realised using manually selected natural points common to the digital images and the point cloud.

Other approaches to registration of freehand photos use colour coded targets placed on the object (Al-Manasir and Fraser 2006), edge extraction algorithms for image and 3D data (Alshawabkeh et al. 2006) or intensity data recorded by the laser scanner (e.g.: Haala 2004; Böhm and Becker 2006; González-Aguilera et al. 2009; Meierhold et al. 2010), though these methods have not been widely implemented in proprietary software.

2.2.2 Helicopter-based laser scanning

In the first step of the helicopter-based data registration the trajectory of the helicopter is reconstructed using the GNSS/INS data and corrected relative to a base station (Vallet 2007). The time stamps of GNSS recordings and inertial data are combined together to obtain the positions and orientations of the laser scanner during the flight. Based on this the laser data can be processed to obtain coordinates of the points in the point cloud. Similarly, time stamp of the image and GNSS/INS data are used to retrieve the positions and orientations of the camera centres (Buckley et al. 2008b).

2.2.3 Image-based modelling

As previously mentioned the relative orientation of the images is performed prior to the 3D data reconstruction from images so at this stage the point cloud and the image data are already registered into a single coordinate system. If required, the local project coordinates can be transformed to a geodetic coordinate system based on position of the ground control points captured in images and surveyed in a geodetic coordinate system.

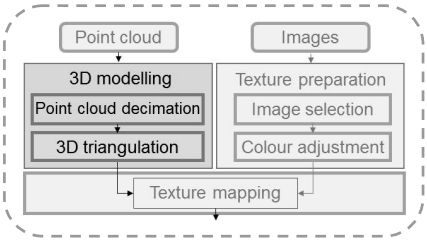

2.3 3D modelling

The result of the described above image- and laser-based surface reconstruction approaches is most commonly a point cloud and a set of images. The size of the dataset depends on the size of the outcrop and the density of the point cloud, but may be millions of 3D points and hundreds of digital images, covering hundreds of meters, or in the case of helicopter-based datasets, tens of kilometres of outcrop.

Known orientation of the images with respect to point cloud allows for determination of an RGB value from covering images for each point in the point cloud. Although a dense point cloud coloured with the spectral (RGB) data may be used for geological interpretation (Buckley et al. 2008a), the discrete nature of such a surface representation may not be suitable for interpretations and measurements at fine scale. Textured 3D models provide high resolution continuous data and therefore are more suitable for interpretations and accurate identification of the fine-scale features (Bellian 2005; Buckley et al. 2008a). Creation of textured 3D models accurately representing complex topography that can be handled by the software and hardware resources requires specific point cloud preparation, i.e. decimation, filtering and representation of the surface geometry by a Triangulated Irregular Network (TIN).

2.3.1 Point cloud cleaning and decimation

In order to ensure realistic texturing, reduce the processing time and guarantee comfort of data handling the point cloud needs to be cleaned and thinned to manageable sizes (Buckley et al. 2010a). This size changes rapidly with hardware and software capabilities.

Points representing vegetation and other unwanted features in the point cloud need to be filtered as they decrease the quality of the surface reconstruction (Section

2.3.2) and cause surface artefacts. Manual point cloud editing is possible, but for outcrops covered with sparse vegetation may be very time-consuming. Rough vegetation filtering can be realised automatically using the spectral (RGB) information in the digital images to classify points in the cloud (Buckley et al. 2010a). The points that have strong intensity in the green channel are likely to represent the vegetation and can be removed from the point cloud based on empirically selected threshold. Other methods for filtration of vegetation employing spatial filters or near-infrared camera are reported in (Alba et al. 2011a).

Because dense point clouds usually contain more points than required for accurate surface triangulation process their thinning is required (Buckley et al. 2010b). In case of the laser-based modelling much redundancy may be present in the areas covered by multiple scans or flight strips. In addition to uniform point decimation, thinning based on surface curvature analysis can be automatically applied so that more points are kept to describe rugged surfaces, and redundant points on smooth surfaces are deleted.

In order to create a textured model the topographic surface needs to be reconstructed and represented by a TIN model. Therefore the cleaned and decimated point needs to be transformed into a triangular mesh.

2.3.2 Triangulation and mesh optimisation

Surface reconstruction from point clouds has been addressed in research for over twenty years starting with the work of Hoppe et al. (1992). An overview and comparison of the most commonly applied meshing techniques can be found in (Berger et al. 2011). Although fully automatic, correct surface reconstruction from unorganised point clouds is a non-trivial task due to range shadows, sharp topography changes, potential vegetation and random errors (Remondino and El-Hakim 2006). Therefore manual mesh editing is required to solve topology problems, improve equiangularity, reorient inverted triangle normals and smooth the surface (El-Hakim et al. 2008; Buckley et al. 2010a). Automatic curvature-based hole filling (e.g. Wang and Oliveira 2003) and simplification of over-sampled areas can be applied to deliver a continuous surface model.

In order to facilitate the texture mapping (Section 2.5) and data handing, larger outcrop models need to be divided at this stage into smaller sections. As in the previous data processing step, this size depends on the hardware and software capabilities.

Another way to facilitate visualisation and handling of very large datasets (e.g. helicopter-based, but not only) is creation of a hierarchical set of Level of Detail (LOD) (e.g. Hoppe 1996) and a spatial segmentation of the entire triangular mesh (Buckley et al. 2008b). Such data handling method allows the viewing software (specifically designed) to load the data in required resolution according to object-to-screen distance (zoom-in level). More details about the solution implemented in the workflow can be found in (Buckley et al. 2008b) and more method background in (Erikson 2000).

The result of this processing step is a continuous surface model represented by a TIN and therefore suitable for texture mapping.

2.4 Texture preparation

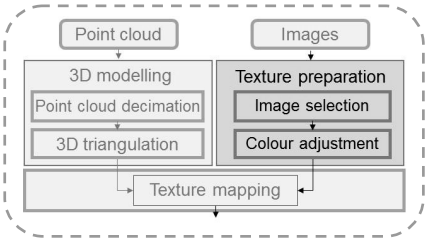

Texture mapping (Heckbert 1986) is a critical step for enhancing visual appearance of the 3D model and requires the relationship between all the mesh vertices and the corresponding image points to be defined. In this process, available registered images are mapped to the 3D model geometry, using the collinearity condition (Wolf and Dewitt 2000) and the image interior and exterior orientation parameters. However, because image sets are collected from multiple locations, with large overlap, and sometimes with different camera or lens configurations, each triangle in the surface model may be visible in several images. An example of redundancy in image data in a helicopter-based dataset is visualised in Figure 2.2, where the mesh triangles are seen in up to 16 images.

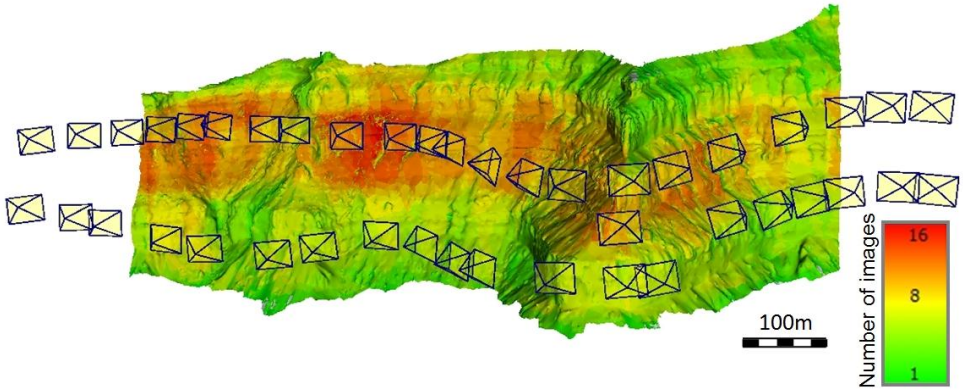

Figure 2.2. 3D terrain model and footprints (navy blue polyhedrons) of acquired images, a section of the Book Cliffs, Utah, USA. Mesh triangles coloured depending on the number of covering images. Output from method presented in this thesis (Paper A).

One way to combine data from multiple images is to blend (e.g. average) all available colours for each pixel of triangle texture (Poulin et al. 1998). Such approach results in a very smooth visual impression, where colour and brightness differences are eliminated, but also in blurring of the data (high frequency information is eliminated), emphasised by erroneous image orientations (El-Hakim et al. 2003; Petsa et al. 2007). In the case of outcrop models, geologists interpret and digitise geological features that can sometimes only be subtly differentiated from their local neighbourhood. Thus it is of high importance to avoid local rendering methods using colour blending between images. Therefore in this workflow only one single image is used as texture source for each mesh triangle (Buckley et al. 2010a).

The currently available automatic texture mapping procedures (Section 2.5) do not necessarily provide the best textured model when using all available photos (Bénitez and Baillard 2009; Buckley et al. 2010a). This is due to distracting texture discontinuity artefacts, which may be caused by small registration errors and incorrect modelling of lens distortion. An example of such artefacts is shown in Figure 2.3. The darker texture patches come from a different image than the rest of the texture in the figure. The positional shift (marked with arrows) between texture samples coming from different images causes artefacts that may disturb measurements and geological interpretations.

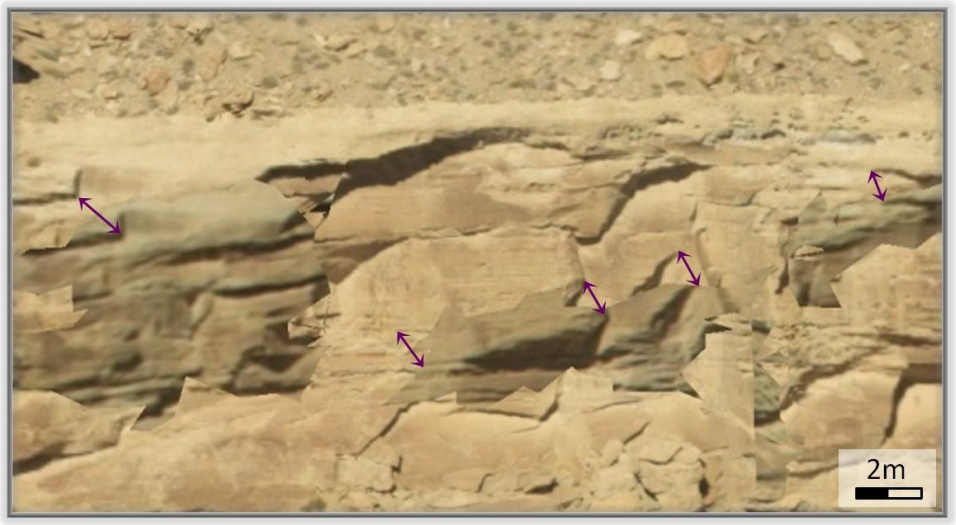

Figure 2.3. Texture artefacts (darker patches) caused by registration errors and imperfect implementation of additional camera calibration parameters in areas covered by multiple images. Texture displacement marked in purple.

Therefore the number of images used in the texture mapping should be minimised where possible.

2.4.1 Image selection

Few studies directly relevant for image sorting are reported in the literature (Haala 2004; Bénitez and Baillard 2009) but developments in research on optimal viewpoint selection in 3D scenes (Vázquez et al. 2001; Snavely et al. 2008; Shirani-Mehr et al. 2009), representing the inverse of the given viewpoints in the texture mapping problem, are also relevant.

In the existing workflow image selection is realised manually, in two stages. Firstly, because in the previous processing step larger models were divided into smaller sections, all images relevant for each model section need to be identified from all the photos collected in the dataset. Secondly, the images most suitable for texturing are manually selected based on the visual (subjective) assessment of geometrical relations between the 3D model and image footprints. The latter step is non-trivial and, especially for models with complex topography, requires the operator to have a good ability in spatial orientation and awareness.

Once a subset of images and future texture candidates is selected, colour adjustment can be carried out to avoid rapid radiometric changes in the photorealistic model.

2.4.2 Image colour adjustment

All images are acquired over a period of time, e.g. during one or several days, and therefore with different lightning conditions. Non-uniform colours of corresponding features in images affect the seams between images in the texture and decrease the level of realism of the photorealistic model.

Three types of radiometric differences can be distinguished: interior image illumination variation (vignetting), global radiometric slope between images, and local illumination differences, e.g. caused by shadows. Vignetting is mainly caused by the optical system and lens characteristics (Sidney 2002). An overview of the available vignetting correction methods can be found in (Goldman and Chen 2005) and (Lelong 2008). Work related to local and global illumination correction for creation of panoramic images is also relevant and reported in (Xiong et al. 2009).

Methods addressing all three sources of the radiometric differences during the texture mapping procedure are presented in (El-Hakim et al. 1998) and (Hanusch 2008). The first work uses an iterative image brightness balancing method analogous to least-squares geodetic height network adjustment. Hanusch (2008) uses a biharmonic spline function in the brightness interpolation for local corrections. The vignetting and global brightness differences are corrected by modification of the L (lightness) component of the images transformed to CIELAB colour space (Bern 2000).

Methods originating in computer graphics, e.g. the tone (Mantiuk et al. 2009) and texture transfer (Efros and Freeman 2001) are relevant as well.

The global and local illumination differences may be also minimized by collecting the images over a very short period of time (El-Hakim et al. 2008), though this is not always practicable.

In the data processing workflow used in this research the colour adjustment is restricted to approximate global balancing, realised manually on the pre-selected

images. Once this task is completed the triangulated surface model can be combined with imagery to create the photorealistic 3D model.

2.5 Automatic texture mapping

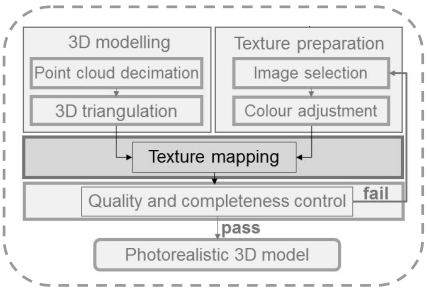

Automatic texturing of surface models from multiple camera images using texture mapping has been addressed for many years (Busch 1991; Niem and Broszio 1995; El-Hakim et al. 1998; Frueh et al. 2004; Abdelhafiz 2009; Iwaszczuk and Stilla 2010). Most of the contemporary algorithms use similar geometric principles for image application to triangles: minimizing the camera - triangle viewing angle and maximizing the effective texture resolution, but additional conditions may be applied, such as triangle reassignment to different images to improve coherence with neighbouring triangles (Frueh et al. 2004). Viewing angle is the angle between the ray passing from camera centre to the triangle centroid, and the normal vector of the triangle (Figure 2.4A). The smaller the viewing angle, the more suitable the image is for texturing. Effective texture resolution is the resolution of the triangle in the image (compare Figure 2.4B and Figure 2.4C), taking into account image resolution, camera lens and the distance to the object.

The optimal texture mapping is realised when a triangle is textured using an image containing the highest number of pixels (highest effective triangle resolution) and taken from a position guaranteeing the smallest camera – triangle viewing angle (Frueh et al. 2004; Buckley et al. 2010a).

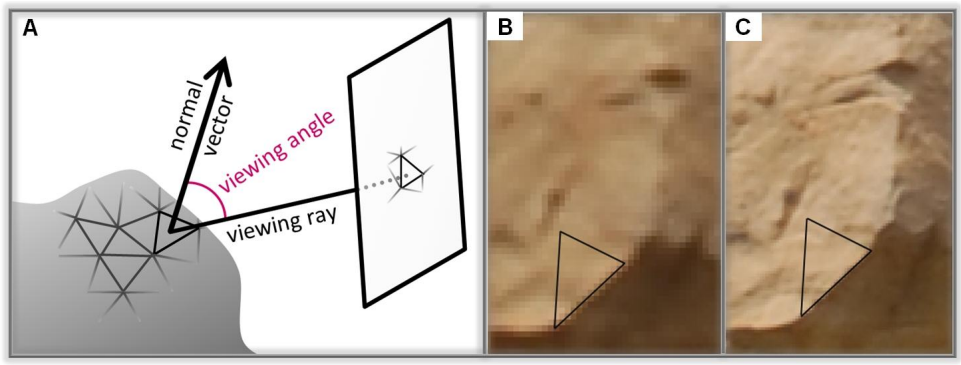

Figure 2.4. Camera – triangle viewing angle (A). Low (B) and high (C) effective triangle resolution within the image.

Although fully automatic, texture mapping can be a very time-consuming task. In cases when for easier data handling and visualization LODs are created for a triangulated model, each level is textured using a different image resolution. For larger model sections this processing step may take several hours of CPU time. Once texture mapping is finished the quality and completeness of resulting photorealistic 3D model needs to be verified.

2.6 Quality control

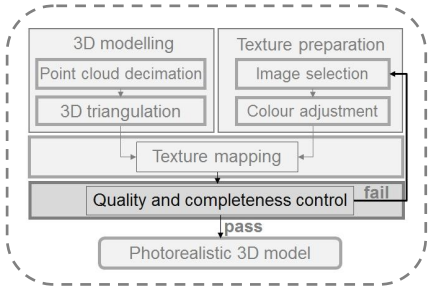

Quality and suitability of the textured model for interpretation and measurements is checked visually. Larger areas of model without texture indicate that an image was missed at the image selection stage (Section 2.4.1). Decreased texture quality (Figure 2.5) might result from the poor image orientation with respect to the model. In cases when low quality or incomplete texture appears in areas of geological interest, realism is disturbed, influencing the interpretation and measurements. The user must be aware of the presence of such artefacts. Where poor quality texture is present, a new image sorting (Section 2.4.1), colour adjustment and texture mapping are

required to be carried out. For large and complex models the cost in processing time of repeating texture mapping may be high.

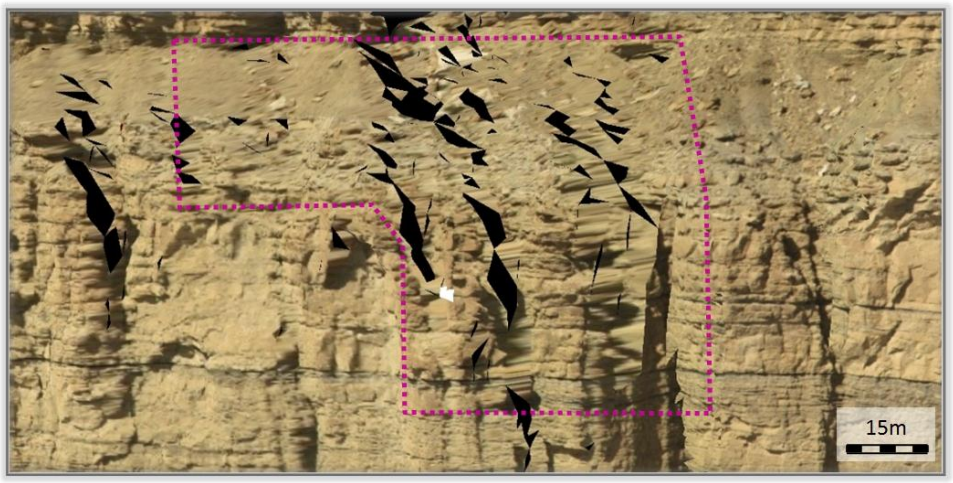

Figure 2.5. An example of a low quality (smeared) texture (marked in purple) resulting from poor image orientation with respect to the terrain model, indicating an image has been missed from those selected for texturing. Black areas denote mesh triangles without texture.

The result of the processing workflow described above is a photorealistic outcrop model ready for visualisation, interpretation and measurement. Due to multiple height (Z) values for each X, Y position, not handled by most of geographical information software, visualisation of large textured 3D models is still problematic. Handling high resolution multi-image textures and LODs requires specific software design. In this research in-house software reported in (Buckley et al. 2008b) was used for visualisation and measurements.

Chapter 3

Integration of 3D models with auxilliary data: Background

In addition to geometry of the object, photorealistic 3D models provide also spectral information contained in the RGB images. Many applications can also benefit from integration of the 3D model with other data. One such example in geosciences is using intensity of the reflected laser signal recorded by the TLS to distinguish different stratigraphic units (Pesci et al. 2008), lithology (Burton et al. 2011), gravel from sandy facies (Klise et al. 2009), surface moisture characteristics (Nield et al. 2011) as well as salt marshes (Guarnieri et al. 2009) and levels of clay content in carbonate rocks (Franceschi et al. 2009). Intensity data can be successfully used to detect and map damages in historical buildings (Armesto-González et al. 2010) and civil engineering structures (González-Jorge et al. 2012).

Integration of the geological outcrop models with data acquired by airborne sensors is also beneficial. Using terrestrial laser scanning to complement a digital surface model derived from aerial imagery, followed by texturing with both: aerial and terrestrial imagery, allowed for tracking of geological, also vertically oriented, strata over large areas (Buckley et al. 2010b). Combination of terrestrial and aerial laser scanning was also successfully used to measure displacements in analysis of landslides mechanisms (Oppikofer et al. 2009).

Complementing virtual outcrop models with elevation data provided by the spaceborne Shuttle Radar Topography Mission (SRTM) and airborne SWIR hyperspectral data allowed exposed dolomitisation patterns to be mapped (Bellian and Kerans 2007). Enhancing satellite Synthetic Aperture Radar (SAR) data covering

large areas in high temporal resolution with high accuracy TLS data was beneficial for studying forest defoliation (Kaasalainen et al. 2010).

Combining data acquired by different close range sensors is also advantageous, e.g. new possibilities for energy inspections of buildings have been provided with the integration of thermal infrared imagery and TLS, giving new ways of qualitative and quantitative characterisation of thermal bridges (Lagüela et al. 2012; Weinmann et al. 2012). The combination of low radar spatial resolution in ground-based radar interferometry, yet high frequency deformation measurement, with TLS geometry gave new possibilities for dam deformation measurements (Alba et al. 2008). Assessment and mapping of structural damage of engineering objects was possible when laser-based models were merged with processed products of ground penetrating radar (Lubowiecka et al. 2011).

A further example of close range data fusion is the use of terrestrial hyperspectral imagery to complement 3D lidar models for geological applications (Kurz et al. 2008; Nieto and Monteiro 2010; Kruse et al. 2012; Kurz et al. 2012). It is this last example that forms the basis for the next section.

3.1 Integration of 3D outcrop models and hyperspectral imagery acquired with HySpex SWIR-320m camera

Hyperspectral imaging is an established method that allows for mapping and quantification of materials indistinguishable by the human eye (Goetz et al. 1985). Hyperspectral sensors capture hundreds of narrow (3–15 nm) spectral bands covering a wide portion of the electromagnetic spectrum. A near-continuous spectral curve that can be created for each image pixel permits detection of subtle geochemical differences, or quantitative analysis of pixel composition (van der Meer and de Jong 2001). Many minerals exist that cannot be distinguished using visible light, but exhibit specific absorption and reflectance properties in the infrared region of the electromagnetic spectrum (e.g. limestone and dolomite) (van der Meer and de Jong 2001). Recent technological advances have introduced portable terrestrial hyperspectral sensors, for example the HySpex SWIR-320m (Norsk Elektro Optikk A/S) camera, adding new possibilities to studies of mineralogy and lithology (Kurz et

al. 2012). Integration of such sensors with terrestrial laser scanning data allows for complementing 3D models with results of hyperspectral data classification and therefore facilitates geological interpretations as well as communication of outputs to users (Slocum et al. 2008).

3.1.1 HySpex SWIR-320m camera

The HySpex SWIR-320m is a portable terrestrial hyperspectral line scanner, with a 14° field of view across track, covered by 320 pixels. The sensor covers the spectral range from 1.3 µm to 2.5 µm over 241 bands, with a sampling interval of 5 nm. As a pushbroom linear-array sensor, the system uses a rotation stage to construct the image in the along-track direction, resulting in a cylindrical imaging geometry. Previous work (Kurz et al. 2011) showed that the sensor can be successfully represented by a geometric model for panoramic cameras (Schneider and Maas 2006). Establishment of the correct sensor model is critical for tasks requiring precise data coupling, such as image orientation or texture mapping.

3.1.2 Integration of hyperspectral and lidar data

In order to integrate hyperspectral imagery with photorealistic 3D models the relation between the 3D model coordinates and the hyperspectral panoramic images needs to be determined. For central perspective RGB imagery similar tasks can be automatically solved by matching digital photos with TLS intensity images (Böhm and Becker 2006; González-Aguilera et al. 2009; Meierhold et al. 2010). However, such an approach relies on the laser scanner intensity recorded with high enough dynamic range to allow an interest operator to be successfully applied.

Nieto and Monteiro (2010) registered the hyperspectral data automatically, based on tie points between a 2D image formed from the coloured (RGB) point cloud and the true colour image composition created from the hyperspectral data. However, the HySpex SWIR-320m does not cover the visible part of the electromagnetic spectrum, so the significantly different spectral appearance of objects in conventional photographs and hyperspectral scans needs to be handled by the image matching algorithm.

A successful method for integration of the data acquired with the HySpex SWIR-320m hyperspectral scanner with lidar and image data was presented in Kurz et al. (2011) and is sketched in Figure 3.1.

In this data integration workflow the relation between the 3D lidar data and the 2D hyperspectral scans is established based on corresponding (homologous) points measured with three different approaches. First, retro-reflective targets (Figure 3.2D) are automatically extracted from the point cloud and identified in hyperspectral imagery using spectral classification and pixel unmixing (Ichokua and Karnielia 1996).

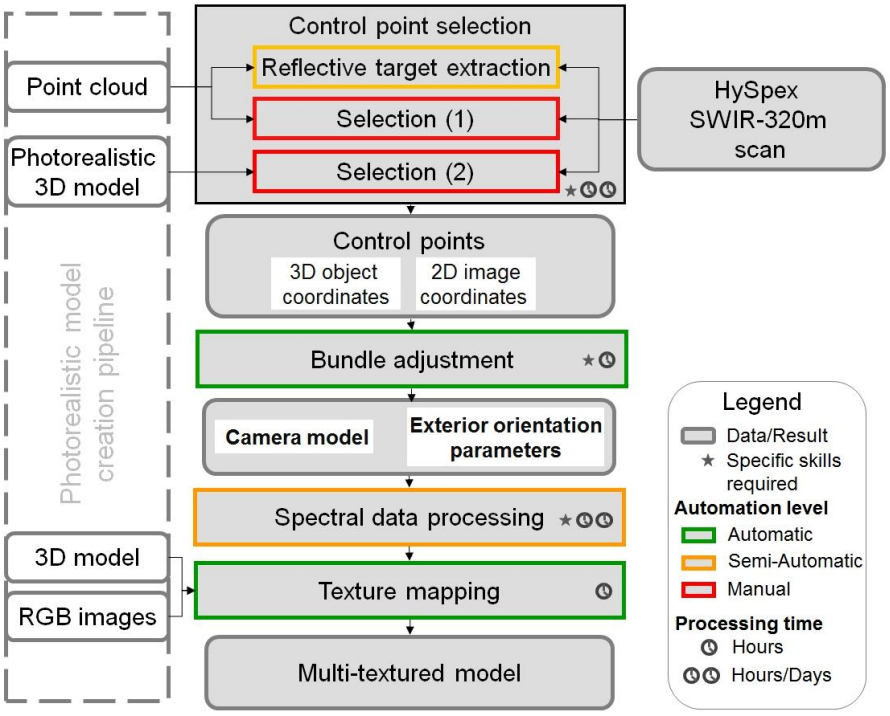

Figure 3.1. Workflow for integration of hyperspectral and lidar data, as described in (Kurz et al. 2011).

Next, natural corresponding points between the point cloud and hyperspectral image are manually selected in order to ensure a uniform point distribution. However, in problematic areas, where identification of such points in the lidar point cloud is

difficult (Figure 3.2A), homologous points are sought between the hyperspectral imagery (Figure 3.2C) and the photorealistic 3D models (D).

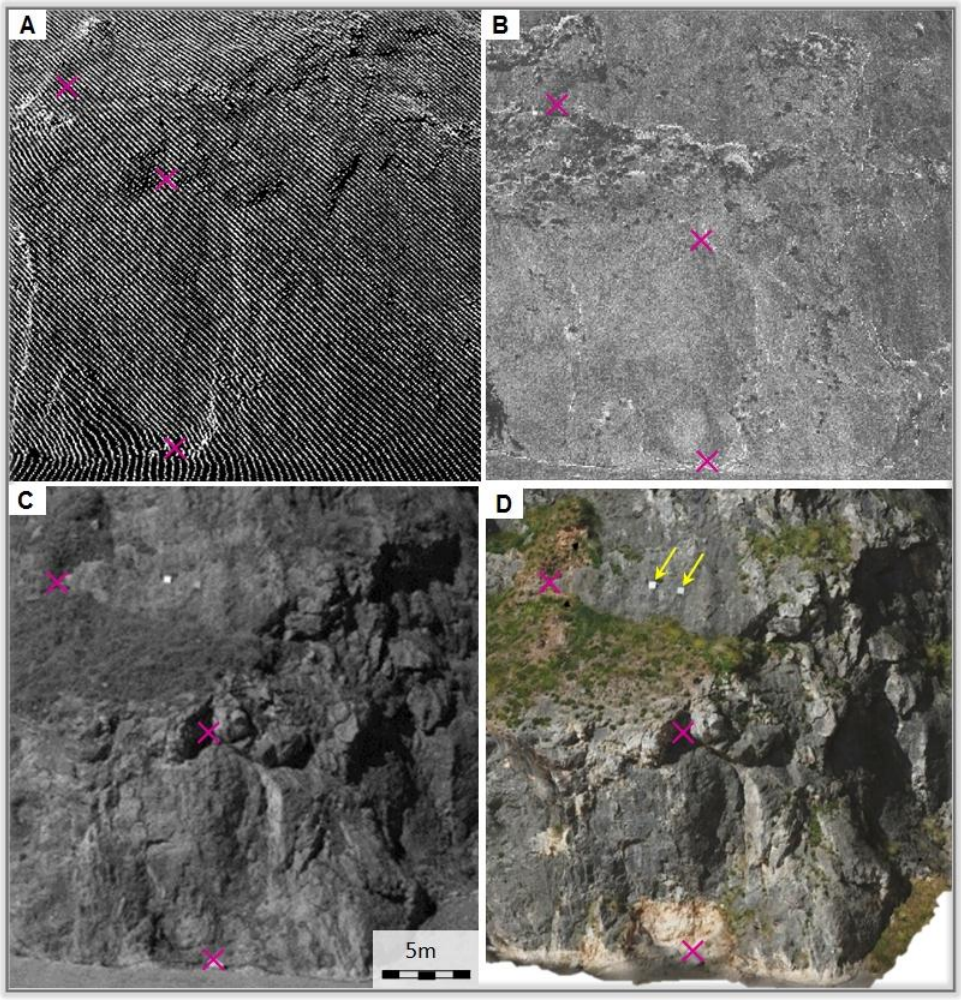

Figure 3.2. Laser point cloud coloured with intensity of the reflected laser signal (A), and the corresponding part of: the 2D image created from intensity values (B), the hyperspectral scan, band 1.336μm (C), and the 3D model textured with RGB images (D). Purple crosses mark homologous points in datasets. Reflective targets marked with yellow arrows.

The 2D image and 3D object coordinates of identified points are transformed to a format suitable for the software Bundle (Schneider and Maas 2007) designed to handle several sensor models, including the geometric model for panoramic cameras

(Schneider and Maas 2006). Exterior orientations of the hyperspectral scans, as well as the intrinsic camera parameters are simultaneously determined in a bundle block adjustment (Luhmann et al. 2007).

Despite the fact that the hyperspectral data acquisition was optimised for geological purposes rather than for photogrammetric processing, and adjacent scans had very little overlap, the hyperspectral data were registered in the TLS coordinate system with a precision of around one pixel. Such data integration quality is more than sufficient for most geological applications.

The established sensor intrinsic and exterior orientation parameters supplied to the collinearity condition with additional parameters (Schneider and Maas 2006) allowed for texturing of the triangulated 3D lidar model with products of spectral data processing, e.g. classification results.

Despite the success of the established data integration workflow the procedure for tie point selection was reported as time-consuming and inefficient for multiple hyperspectral scans (Kurz et al. 2011). The obstacles impeding the manual tie point selection process were mostly related to characteristics of the lidar data such as the discrete nature of the point cloud (Figure 3.2A) and low dynamic range of the intensity values recorded by the specific laser scanner used (Riegl LMS-Z420i). The latter can be observed in A and B, where all materials represented by the point cloud have very similar intensity. Identification of homologous points between the hyperspectral data and the textured 3D model was much easier, but the relatively low spatial resolution of hyperspectral data and the different visible appearance of data captured at different wavelengths (Figure 3.3) affected the accuracy of point localisation.

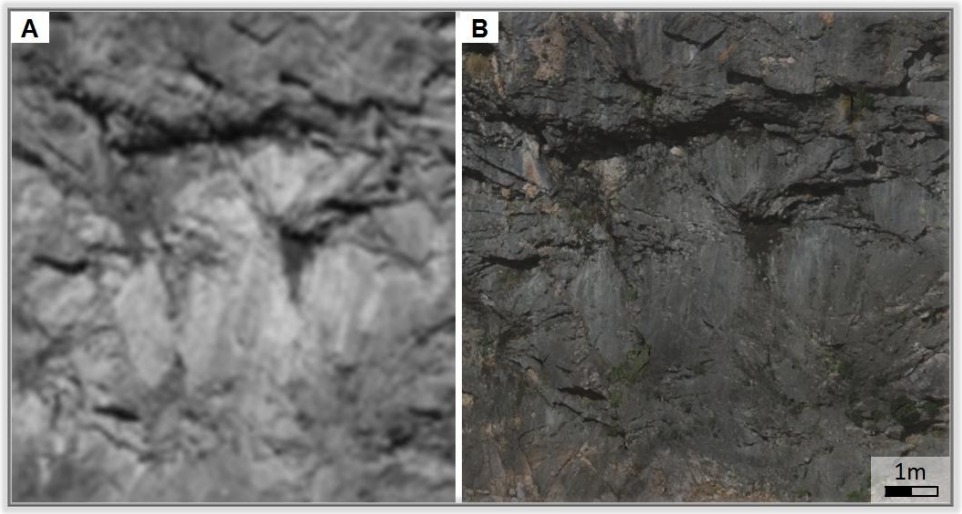

Figure 3.3. (A) Sample of a hyperspectral scan, band 1.336μm and (B) the corresponding area of the photorealistic model.

Chapter 4

An improved workflow for image- and laser-based virtual geological outcrop modelling

The main goal of the work presented in the thesis was to make the data processing workflow more accessible for users from outside of the geomatics domain. In order to achieve that, two steps of photorealistic models creation process requiring manual work and a degree of technical background in geomatics were addressed (Figure 1.3). New procedures and frameworks were developed in order to increase the automation level and facilitate the required user input in the process of image selection prior to texture mapping (Section 2.4.1) and the process of tie point selection between the 3D data and hyperspectral imagery in the data integration workflow (Section 3.1.2).

Developments related to image selection for optimised texturing of 3D models are presented in Paper A and Paper B. The first publication reported preliminary study results and presented the general problem with a focus on the visual assistance in image subset selection and increase of users' confidence in the quality of the selected image set. The proposed new quality measures and evaluation of the automatic image sorting algorithms extend the work and are described in Paper B.

The work on semi-automatic method for integration of terrestrial hyperspectral imagery with lidar and image data is reported in Paper C, Paper D and Paper E. Paper C presents a skeleton of the final, mature data integration workflow described in Paper D. Paper E documents optimisation of the automatic tie point matching routines.

Because the included Papers are by nature disjointed, the following sections summarise the performed research, highlighting the contributions made in this thesis.

4.1 Image selection for optimised texturing

Selection of an optimal subset from a global image set requires complex spatial analysis of multiple variables. Manual image selection, based on examining of the image footprints towards the 3D model can be challenging and time consuming, especially for large models covering rugged terrain, where the user must account for occlusions and ensure that image overlap is sufficient to cover relevant model triangles. This makes the following data processing steps iterative (Figure 2.1), as a missed image, or poor orientation with respect to the model, will require a new sorting and texture mapping to be carried out.

To address this, a framework was developed for computer-assisted image geometry analysis and subset selection for geometrical optimisation of texture quality in photorealistic models. The visual assessment of the image–3D model visibility check used in the manual image selection method was substituted by a plane–line intersection test based on geometrical dependencies between the images and model triangles. Several objective quality measures were adopted and new indicators were proposed (Paper B) to guide the user decision in the image selection process. Because in the spatial domain analytical quality indicators, expressed purely numerically, may be insufficient to convey the necessary decision making information to users (MacEachren and Ganter 1990), they were supplemented with visualisations of quality measures, such as colour-coded quality maps, tables and plots, facilitating understanding of complex spatial problems (Slocum et al. 2008). Automatic image sorting algorithms originating in computer science and information theory were proposed and implemented to quickly provide the user with candidate image subsets.

4.1.1 Numerical quality measures

Assessment of the texture quality in photorealistic models is complicated by their heterogeneous nature, because different parts of the model may have widely varying qualities. Therefore such assessment needs to be performed at the model triangle level. In order to realise that two primary quality measures, considered by most of the contemporary texture mapping algorithms (El-Hakim et al. 1998; Frueh et al. 2004; Abdelhafiz 2009; Iwaszczuk and Stilla 2010), and described in Section 2.2.5, were

adopted in this work: camera–triangle *viewing angle*, and effective resolution of the triangle in the image, expressed by *scale*.

As previously mentioned, computations of effective resolution of the triangle in the image take into account image resolution, camera lens and the distance to the object. The result can be understood as a number of pixels representing a triangle in the image. Images providing the highest number of pixels for a triangle are preferred, if their *viewing angle* is not too oblique. In order to ease comparison and handle significant differences in effective resolution of a triangle visible in covering images, the values are mapped into the range $[1, \infty)$ so that the image with the highest effective resolution (best) gets a value equal to one. To highlight this operation and avoid confusions, name of this quality measure was changed to *scale*. A lower effective triangle resolution results in an increase in scale. For example, a scale equal to two denotes a twice worse effective triangle resolution than in the best available image. An analogous procedure is applied to the (sine of the) *viewing angle*, resulting in normalised viewing angle used to compute image and texture quality indicators.

Image suitability for texture mapping

The primary texture measures are used to numerically express image suitability for texture mapping with average values of *viewing angle* and *scale* for all triangles contained within the image. A supplementary measure, *image quality*, is introduced in order to provide a single quality value per image. *Image quality* is computed as the average product of the normalised *viewing angle* and *scale* parameters and, analogously to *viewing angle* and *scale*, smaller *image quality* values denote higher image suitability for texturing.

Texture quality indicators

As mentioned in Section 2.4, in areas covered by multiple images, texture quality may be affected by small registration errors causing disturbing texture artefacts (Figure 2.3). In the existing processing workflow this problem is addressed by minimizing the number of input images, which in turn can be seen as data or information loss. To support the user decision upon the final trade-off, the

geometrical data/quality loss is estimated and provided in a form of three indicators: *angle loss*, *resolution loss* and *information loss*.

The *angle loss* (viewing angle) and *resolution loss* (scale) are computed for a set of images as the root mean square of discrepancies with respect to the hypothetically best achievable geometrical texture quality, realised when a 3D model is textured with all available images. In such case, triangles are textured using the most suitable parts of all available images. In other words, all the information contained in the images is utilised and therefore *angle loss* and *resolution loss* would equal zero.

The *information loss* was defined as an average ratio between the product of the normalised *viewing angle* and *scale* parameters resulting from the current image subset, and the analogous value computed using all the available images. An *information loss* value equal to two denotes twice worse average texture quality indicators compared to the model textured with the full image set.

Additionally, the geometric texture quality resulting from a selected image subset was described by numerical indicators such as average and median values of *viewing angle* and *scale*.

4.1.2. Visual guidance to support decision

In order to facilitate the understanding of geometrical relationships between the triangular model (Figure 4.1A) and the covering image set (Figure 4.1B), static and interactive information visualisation methods (Ware 1999), in the form of 2D and 3D quality maps, tables and plots in linked views were employed. The application was implemented in C++ and used the OpenSceneGraph library (Wang and Qian 2010) for 3D scene handling, and Qt4 (2012) for graphical user interface control.

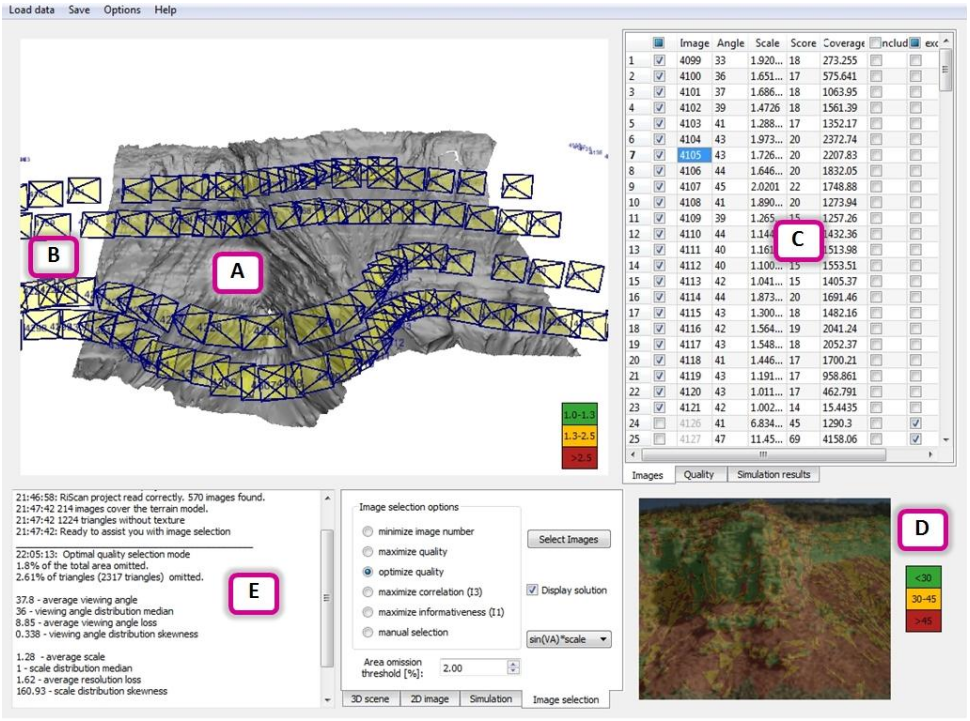

Figure 4.1. Framework for visualisation and analysis of texture parameters. The 3D scene is composed of a 3D model (A) and footprints of the overlapping images (B). Numerical image quality indicators are reported in a table (C) and as a colour-coded map (here: the viewing angle) overlaid on the original image thumbnail (D). Numerical texture quality indicators are reported in a log window (E).

Image suitability for texture mapping

To supplement the average image quality indicators, a colour coded map of the *viewing angle* and *scale* computed for all triangles seen by the image can be displayed. Alternatively, this colour map can be overlaid on the original image thumbnail (Figure 4.1D). This visualisation provides indicators of local data quality and enables the user to quickly understand which parts of the image are most suitable for model texturing.

Texture quality indicators

Visualisation of the predicted model texture quality enables the user to identify spots on the 3D model where quality may be reduced. Therefore the 3D model can be

coloured with a map of classified predicted *viewing angle*, *scale* and *information loss* (Figure 4.2). Additionally, the area of the 3D model with *information loss* corresponding to high, medium and low quality texture is quantified and presented to the user as a percentage of the total textured model area. These areas can then be refined by adding images to the image subset prior to texture mapping, thus avoiding having to repeat the time-consuming processing.

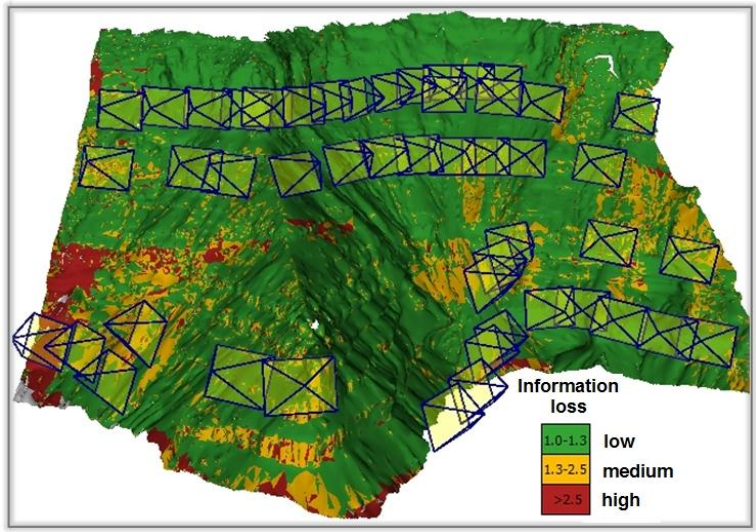

Figure 4.2. 3D model coloured with a map of classified predicted information loss. High, medium and low quality texture marked with green, yellow, red colour coding.

Texture completeness

The developed application allows for control of texture completeness in two ways. Firstly, image ground coverage may be displayed for one or several images, highlighting the relevant triangles of the 3D model (Figure 4.3A). Secondly, when assessing the quality of the currently selected image subset, areas that will not be textured are highlighted (Figure 4.3B). This enables the user to verify if the size and location of the areas without texture are significant and acceptable prior to running the texture mapping algorithm.

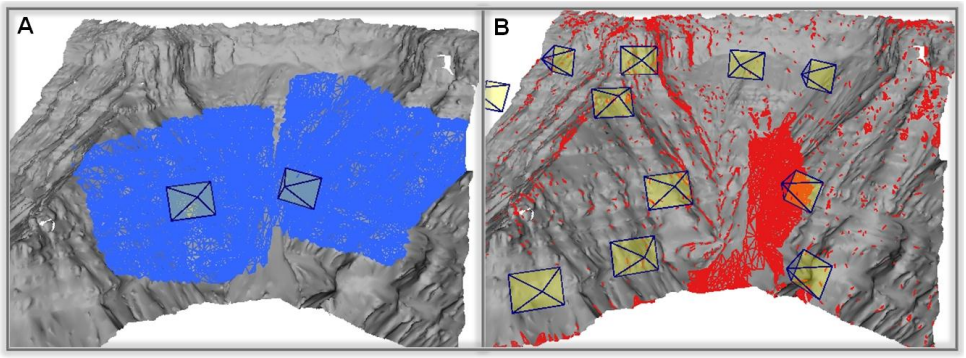

Figure 4.3. Two ways to control texture completeness: by highlighting image ground coverage (A), and by highlighting triangles not covered (without texture) by an image subset (B).

In order to provide the user with an alternative insight into the quality of the selected image subset, the proposed quality measures are also presented in a form of histograms and plots (Paper B).

4.1.3. Automatic image sorting procedures

The visual and numerical quality indicators guide the user in selecting image subsets covering the entire model. However, a more efficient solution is to use the numerical indicators in automatic image selection procedures, to quickly ascertain suitable subsets that can be manually refined before texturing. Therefore three algorithms originating from the field of computer vision (*Optimizing Texture Quality*) and information theory (*Maximizing Information* and *Maximizing Correlation*) were proposed and implemented in the presented framework. The image subsets provided by the automatic procedures were compared to manually selected sets and their suitability for 3D model texturing was assessed. The algorithms and results of the comparison are presented in details in Paper B.

Irrespective of the chosen algorithm, the coverage of the automatically selected images is controlled by defining the maximum allowable percentage of the model without texture. The user can force inclusion (or exclusion) of specific images in the image subset during processing.

4.1.4. Results and discussion

To evaluate the usefulness of the presented framework to domain specialists in geology, three users experienced with the manual image selection workflow, were asked to use the newly developed framework for image selection and provide their feedback. Anecdotal evidence obtained from the user's feedback (Paper A) indicated increased confidence in the final textured model quality and completeness, and shorter time spent on image selection. This suggests that supplementing analytical predicted texture quality parameters with spatial quality maps displayed in an interactive environment facilitates understanding of local texture quality changes.

Results obtained by the automatic image selection algorithms, presented in detail in Paper B, indicate that the automatic image sorting is a valid alternative to manual methods. The *Optimizing Texture Quality* algorithm delivered image sets closest to the quality and size of the manually-selected sets. The automatic image selection methods originating from information theory also provided promising results. However, because the implemented algorithms are purely analytical, they do not control the spatial distribution of the texture quality or untextured areas. Therefore the image subset resulting from the automatic selection procedures should always be verified using the described visual aids and, if necessary, refined manually.

The improved workflow for creation of virtual outcrop models resulting from this contribution is presented in Figure 4.4. Enabling the user to identify regions with low predicted quality or missing texture allows the image set to be refined prior to starting time-consuming texture mapping procedures, and reduces the need for data re-processing and the overall processing time. Nonetheless the quality of the photorealistic models needs to be verified because influences such as varying lighting conditions and data registration errors are not considered in the image selection framework and should be addressed in future work.

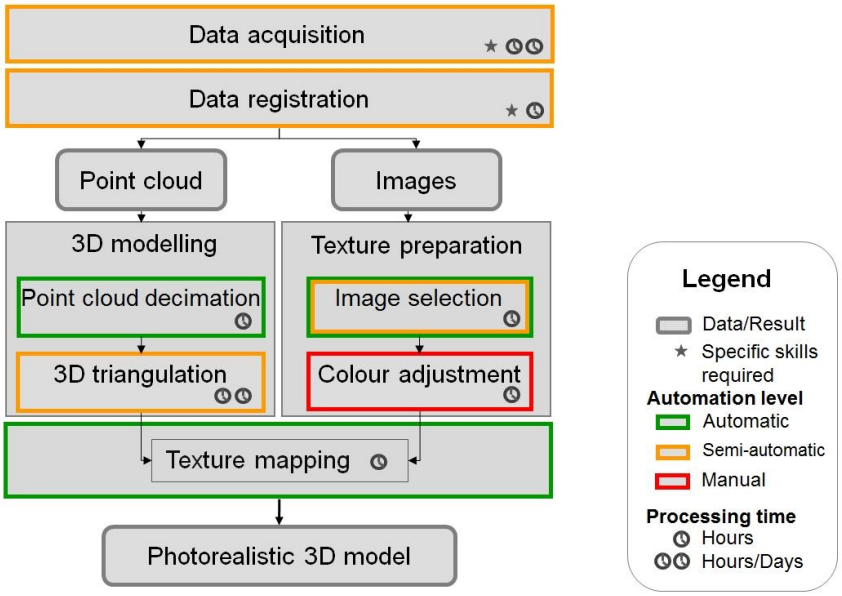

Figure 4.4. Improved workflow for creation of virtual outcrop models.

More work is required to automate the classification of predicted texture quality measures. At the moment the thresholds for the three classes: high (green), medium (orange) and low (red) quality are set up empirically and can be adjusted by the user. Automation of this process would be of great benefit and facilitate processing of datasets with different geometrical characteristics.

Obtaining more user feedback is desirable in order to assess and improve the visualisation effectiveness. Code optimisation is also required in order to handle large terrain models at full resolution.

Finally, several practical issues need to be discussed. In texture mapping the texture can be considered as a mosaic of all relevant parts of the input images. As previously mentioned, most of the texture mapping algorithms use similar principles, minimizing the viewing angle and maximizing the effective texture resolution. However in most of the cases the two criteria are not fulfilled simultaneously, for example an image providing the best effective triangle resolution (*scale* equal to 1) does not necessarily represent the best (smallest) *viewing angle*. Different prioritisation criteria for the two measures are implemented in different software. In order to reliably predict the texture quality, criteria identical to those applied by the

final texture mapping algorithm must be used when computing quality indicators. Therefore whenever a new texturing approach is used (e.g. new software incorporated into the data processing workflow) the exact texture mapping algorithm should be added to the framework presented in this chapter. Precise texture mapping description with sufficient level of details to reproduce the algorithm is critical in such cases, but unfortunately rarely found in the literature.

It is worth stressing that although the framework was so far used in creation of geological outcrop models, it is equally applicable to other disciplines benefiting from photorealistic 3D outcrop models, such as cultural heritage conservation, digital archaeological inventory or city modelling.

4.2 Semi-automatic integration of laser and image data with auxiliary imagery

The second data processing step addressed in this research was the manual selection of homologous points between the laser data and the hyperspectral scans in the workflow for data integration described in detail in Section 3.1.2. As outlined (after Kurz et al. 2011), this process can be very time-consuming and requires skills in data and image interpretation, especially in natural rock exposures. In addition, further challenges are brought about due to differences in sensor geometry, spectral range and spatial resolution. Experiences show that the lack of time to learn about new methods is an important barrier to new techniques being widely adopted by other domains (Butler and Sellbom 2002). Therefore increased automation of the workflow for integration of the hyperspectral and laser data is required to facilitate adoption of the terrestrial hyperspectral techniques in geology.

4.2.1 Semi-automated data integration workflow

Due the very low dynamic range of the point cloud intensity values recorded by the LMS-Z420i scanner used in this work, and relatively homogenous reflectivity of the weathered rock surfaces, it was not possible to create a synthetic intensity image (as e.g. in (Meierhold et al. 2010)) with quality high enough for interest point extraction. Instead, the Nikon images acquired together with the lidar data and registered in the

TLS coordinate system were used as the reference dataset, and hyperspectral panoramas were matched with these. Automatic matching between hyperspectral scans and the digital images allowed establishing the image to image correspondence (2D-2D). Because the digital images were registered in the 3D model coordinate system, the geometric relationship between the 2D image and 3D object (model) coordinates could be derived using the central perspective camera model and the collinearity condition (Luhmann et al. 2007). Once the 3D object coordinates of the points matched between hyperspectral data and Nikon images are established, they can be used as control points in a bundle adjustment.

The procedure summarised above, and presented in details in Paper D, substitutes the manual control point selection. The subsequent processing steps were implemented in C++ and make use of the OpenCV library (Bradski and Kaehler 2008) thus the input files for the Bundle software are created automatically. The exterior orientation parameters of the hyperspectral data and, optionally, depending on the number of images and their configuration, the intrinsic parameters of the panoramic camera can be derived and the following processing steps, i.e. spectral data processing and texture mapping can be completed as described in (Kurz et al. 2011). The resulting new data integration workflow is presented in Figure 4.5.

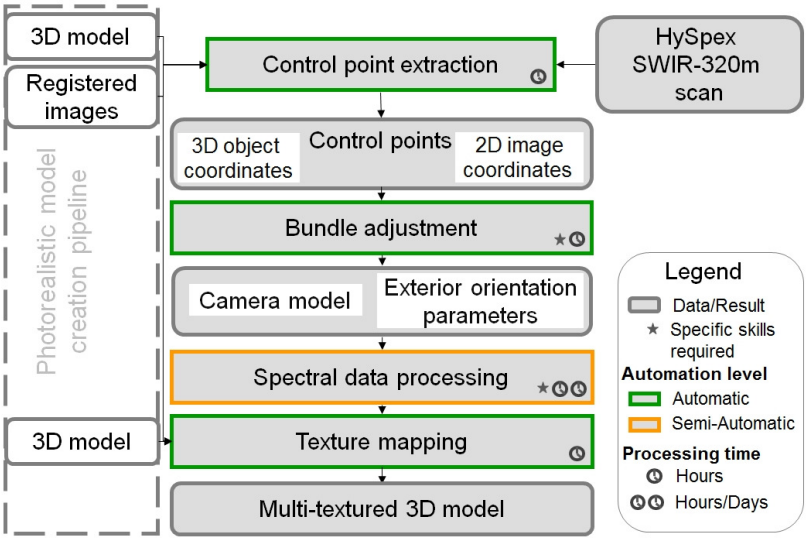

Figure 4.5. Workflow for semi-automatic integration of laser and image data with HySpex SWIR-320m imagery

In the preliminary approach to the automatic control point extraction, presented in Paper C, a single hyperspectral band was used in the automatic image matching process. This method provided relatively few control points and no points that were common to multiple hyperspectral scans. Therefore the exterior orientation parameters were established using space resection. In the space resection the fixed control points are used to determine the orientation of a single scan (Luhmann et al. 2007). Although results of this data integration were satisfactory for geological applications, the hyperspectral data can be registered much more precisely if the exterior orientations are determined simultaneously for all the scans in a bundle solution (Luhmann et al. 2007). Another benefit of the bundle block adjustment is the possibility to establish/check the intrinsic sensor orientation parameters.

However, reliable data integration using bundle adjustment requires a high number of control points common to multiple scans and a uniform distribution of points within each scan (Luhmann et al. 2007). In order to increase the chances of finding points common to two or more scans, maximisation of the number of points automatically found in each panoramic scan was required. In the work presented in Paper D this problem was addressed in two ways: by optimisation of the matching algorithm performance and by using multiple hyperspectral bands in the matching process.

Optimisation of the image matching performance

Finding corresponding points between images acquired in significantly different spectral ranges, i.e. in visible light (Nikon D200 photos) and the short wave infrared spectrum (HySpex SWIR-320m imagery), acquired from slightly different position, in different resolutions and projections can be challenging even for the human eye (see Figure 3.3). Therefore a suitable image matching algorithm was required. Such an algorithm should not only overcome the abovementioned challenges but also provide a sufficient number of points required to precisely register the cylindrical hyperspectral scans (Luhmann et al. 2007). Therefore the Scale Invariant Feature Transform (SIFT; Lowe 1999), reported as robust to difficult geometric and

radiometric conditions (Wessel et al. 2007; Khan et al. 2011; Lingua et al. 2009), was employed.

Because relatively few points were matched when using the SIFT parameters suggested by Lowe (2004), the values of several SIFT parameters were optimised to yield the high number of homologous points required for data integration using bundle adjustment. Although the SIFT is one of the most frequently employed operators (Lingua et al. 2009), and it is natural that in every process the choice of parameter values affects the achieved results, the influence of the SIFT parameters is not reported in the literature in sufficient detail. Therefore the optimisation process, together with a discussion of the influence of different SIFT parameters on the results of matching SWIR and VIS imagery was documented in Paper E.

Band selection

Hyperspectral images consist of hundreds of spectral bands and the SIFT detector operates on a single image band. However, due to the varying appearance of an object at different wavelengths, different sets of interest points are matched in different bands (Figure 4.6).

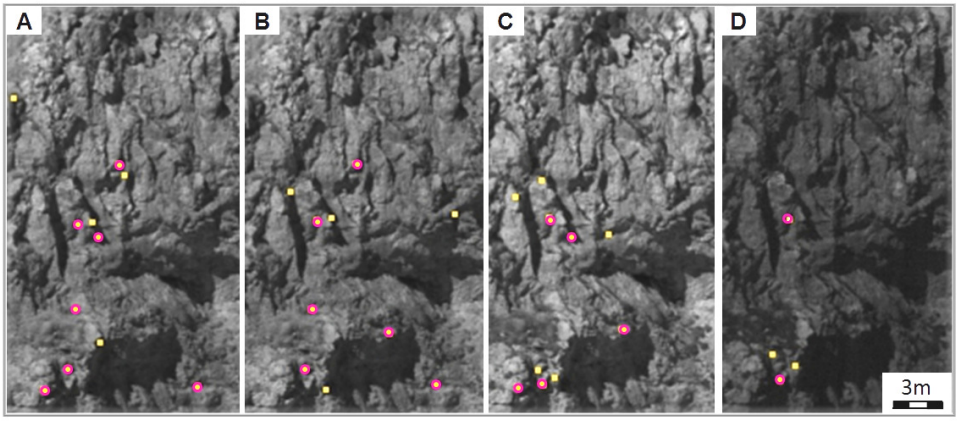

Figure 4.6. Points matched between digital images converted to grayscale and band 1: 1.336μ (A), band 3: 1.346μ (B), band 60: 1.624μ (C) and band 240: 2.502μ (D) of the hyperspectral scan. Points matched in more than one band marked in purple.

This suggested that using multiple bands in the matching process will increase the number of resulting control points. Although matching more than two hundred hyperspectral bands with each covering photo is feasible, it is also inefficient and time-consuming. Therefore an evaluation of the suitability of three different band prioritisation methods was performed and is presented in detail in Paper D. The proposed method for band selection, based on entropy and systematic sampling, enabled the input imagery to be minimised prior to point extraction and matching.

4.2.2 Results and disscussion

Results obtained for two case studies indicated that the proposed method is capable of registering panoramic scans and determining the camera model with accuracy comparable to the manual data integration approach, and sufficient for geological applications.

Success of the data integration method relies on a high number of control points being extracted. In the two examined datasets, using the SIFT operator with optimised parameters and additional outlier elimination allowed between 4 and 22 times more control points to be found than when using the default parameter values. Using multiple bands of the hyperspectral scan allowed a further increase in the number of extracted control points. In result more points common to multiple scans were found and the bundle adjustment could be applied.

A key advantage of the workflow is the reduced user interaction, making it more accessible for non-photogrammetrists as well as shortened overall processing time.

Further developments are required to increase the number of control points in low-textured areas and therefore improve the point distribution within the hyperspectral scan for improved registration quality.

Because the proposed workflow relies on correct integration between the SLR camera and the laser scanner, another way to further increase the data integration quality is to automatically extract points common to all the data acquired by different sensors in the dataset, i.e. the hyperspectral scanner, SLR camera and laser scanner, and use them as control points in a bundle adjustment. Such an approach would allow for simultaneous computation/readjustment of interior and exterior orientation

parameters of the sensors and therefore for more precise data integration. However in order to automatically match points between the laser scanner data and imagery, the reflected laser intensity should be recorded with a dynamic range sufficient to create an image suitable for automatic matching purposes.

Currently, hyperspectral data are collected for the purposes of the end application, and the method should be tested further for datasets optimised for photogrammetric data processing, and optimally with surveyed ground control points available for quality assessment.

Although the semi-automated data registration workflow was initially developed to register cylindrical panoramic scans into the TLS coordinate system, the method is equally applicable to imagery acquired with other sensors, as long as the correct geometric model is supported, and corresponding points can be matched between these imagery and overlapping digital photos. For example the additional free-hand photos (see Section 2.2.2), acquired from a position other than the laser scanner position, can potentially be registered using the proposed workflow. However more work is required to estimate if the registration accuracy is sufficient for high resolution imagery.

Little by little, one travels far.
J. R. R. Tolkien

Chapter 5

Conclusions and future work

The aim of this thesis was to make the existing workflow for creation of photorealistic 3D models and integration with terrestrial hyperspectral data more accessible for users from outside of the geomatics domain. This goal has been reached by addressing limitations in two previously manual processing steps, where most background in geomatics and experience was required: image selection prior to texture mapping and control point selection in hyperspectral and lidar/digital image integration. Techniques originating in such fields of science as geomatics, photogrammetry, computer vision, visualisation and information theory were employed to provide the following individual contributions to the two addressed workflow limitations:

1. Computer assisted image selection prior to texture mapping:

   a) description of texture quality with several new measures, allowing for comparison of the suitability of different image sets for texture mapping purposes;
   b) a new interactive framework providing analytical and graphical assistance in selection of an image subset for geometrically optimised texturing in photorealistic 3D models;

c) increased user confidence in the quality of the resulting photorealistic models, achieved using interactive visualisations and spatial quality maps, and confirmed by anecdotal evidence;
d) automated image sorting algorithms capable of providing image sets for texture mapping, either for direct input, or refinable by the user;
e) reduced photorealistic 3D outcrop creation time obtained by prediction of the texture quality and completeness prior to texture mapping and therefore eliminating the potentially iterative process of image set adjustment encountered in the case of the existing manual image selection approach.

2. Semi-automated registration of terrestrial panoramic hyperspectral imagery with the laser and image data:

a) reduced user interaction obtained by automation of the control point extraction procedure;
b) shortened data integration time realised by automation of the control point extraction process;
c) band selection method dedicated to maximise the number of matched points while minimizing the processing time;
d) confirmation that the SIFT operator can be successfully used in matching images acquired in SWIR and VIS parts of the electromagnetic spectrum;
e) documentation of the influence and importance of several SIFT parameters on the matching results.

Despite these results, more work is required to further facilitate creation of the photorealistic outcrop models and integration with other data and overcome the remaining workflow limitations. In the workflow used in this research, automation of the image colour adjustment is not carried out, but should be addressed to improve the visual appearance of models. Several techniques for global and local colour balancing were recently proposed (listed in 2.4.2), but their suitability should be carefully evaluated keeping in mind that geological features are often identified based on very subtle colour changes; thus the colour adjustments should be applied

moderately. The methods for filtering of vegetation in the point cloud (Section 2.3.1) require more work to improve their efficiency. Further improvements are desired to minimise the co-registration errors between the laser and image data, and therefore improve the coherence between the texture and the 3D model. Registration of freehand photos remains cumbersome and it should be tested if the proposed and implemented routines for semi-automated integration of panoramic hyperspectral imagery with laser and image data provide sufficient accuracy for registration of high resolution digital imagery. Although in this research geological applications have been targeted, it is also applicable to other fields.

With the rapid developments in laser scanning, sensors continuously improve with respect to rates of data capture, data acquisition range or number of recorded pulses. Fully automated methods allowing for terrain reconstruction from images are also progressing and several solutions are already available, also as open source packages (e.g.: Wu (2012) or Astre (2012)). The slowly decreasing cost and increased data processing automation make these technologies more accessible in many applications. One of the impeding factors in fast adoption of photorealistic 3D model creation pipelines, especially for users from outside of geomatics, is a lack of standard terminologies, specifications and methods for performance benchmarking, resulting in difficulties to select a solution fit for purpose. The ability to interact with, interpret and measure huge 3D textured models is a continuing problem. Model sizes and texture resolutions are increasing but both hardware and software still limit possibilities for the interactive visualization of detailed photorealistic 3D models of large areas (Remondino 2011).

Irrespective of the abovementioned obstacles photorealistic 3D models are a great source of geospatial data and it is hoped that facilitated access to the tools and methods for creation of the virtual models, will ease their adoption not only in other science disciplines, but also in daily life, e.g. for educational purposes in geosciences, climbing safety trainings or multimedia museum exhibitions.

References

Abdelhafiz, A. 2009. “Integrating Digital Photogrammetry and Terrestrial Laser Scanning. Ph. D. Dissertation.”

Aguilera, D. and J. Lahoz. 2006. “Laser Scanning or Image-based modeling?A Comparative Through the Modelization of San Nicolas Church.” *International Archives of the Photogrammetry, Remote Sensing and Spatial Information Sciences* 36 (5): 1–6.

Akca, D. 2003. “Full Automatic Registration of Laser Scanner Point Clouds.” *Optical 3-D Measurement Techniques* I: 330–337.

Al-Manasir, K. and C. Fraser. 2006. “Automatic Registration of Terrestrial Laser Scanner Data via Imagery.” *IAPRS* XXXVI: 26–31.

Alba, M., L. Barazzetti, M. Scaioni and F. Remondino. 2011a. “Automatic Registration of Multiple Laser Scans Using Panoramic RGB and Intensity Images.” *International Archives of the Photogrammetry, Remote Sensing and Spatial Information Sciences* 38 (5) (September 3): 49–54.

Alba, M., L. Barazzetti, F. Roncoroni and M. Scaioni. 2011b. “Filtering Vegetation from Terrestrial Point Clouds with Low-cost Near Infrared Cameras.” *Italian Journal of Remote Sensing* 43 (2) (June 30): 55–75.

Alba, M., G. Bernardini, A. Giussani, P. Paolo, F. Roncoroni and M. Scaioni. 2008. “Measurement of Dam Deformations by Terrestrial.” *International Archives of the Photogrammetry, Remote Sensing and Spatial Information Sciences* 37 (B1): 133–139.

Alshawabkeh, Y., N. Haala and D. Fritsch. 2006. “2D-3D Feature Extraction and Registration of Real World Scenes.” *International Archives of the Photogrammetry, Remote Sensing and Spatial Information Sciences* 36 (5): 32–37.

Armesto-González, J., B. Riveiro-Rodríguez, D. González-Aguilera and M. Rivas-Brea. 2010. “Terrestrial Laser Scanning Intensity Data Applied to Damage Detection for Historical Buildings.” *Journal of Archaeological Science* 37 (12) (December): 3037–3047.

Artese, G., V. Achilli, G. Salemi, and A. Trecroci. 2004. “Automatic Orientation and Merging of Laser Scanner Acquisitions Through Volumetric Targets: Procedure Description and Test Results.” *International Archives of Photogrammetry, Remote Sensing and Spatial Information Sciences* 35: 210–215.

Astre, H. 2012. “SFMToolkit.” http://www.visual-experiments.com/demos/sfmtoolkit/.

Barazzetti, L., F. Remondino, M. Scaioni and R. Brumana. 2010. “Fully Automatic UAV Image-based Sensor Orientation.” *International Archives of the Photogrammetry, Remote Sensing and Spatial Information Sciences* 38 (1): 1–6.

Barnea, S. and S. Filin. 2007. “Registration of Terrestrial Laser Scans via Image Based Features.” *Methodology*: 32–37.

Bellian, J. 2005. “Digital Outcrop Models: Applications of Terrestrial Scanning Lidar Technology in Stratigraphic Modeling.” *Journal of Sedimentary Research* 75 (2) (March 1): 166–176.

Bellian, J. and C. Kerans. 2007. “Analysis of Hyperspectral and Lidar Data: Remote Optical Mineralogy and Fracture Identification.” *Geosphere* (6): 491–500.

Berger, M., J. Levine, G. Nonato, L. Taubin and C. Silva. 2011. *An End-to-end Framework for Evaluating Surface Reconstruction*. Scientific report. Salt Lake City, Utah, USA.

Bern, Roy S. 2000. *Billmeyer and Saltzman’s Principles of Color Technology*. 3rd editio. Wiley-Interscience.

Besl, P. J. and H. D. McKay. 1992. “A Method for Registration of 3-D Shapes.” *IEEE Transactions on Pattern Analysis and Machine* 14 (2): 227–241.

Bradski, G. and A. Kaehler. 2008. *OpenCV. Computer Vision with the OpenCV Library*. 1st ed. O’reilly.

Buckley, S. J., H. D. Enge, C. Carlsson and J. A. Howell. 2010. “Terrestrial Laser Scanning for Use in Virtual Outcrop Geology.” *The Photogrammetric Record* 25 (131): 225–239.

Buckley, S. J., J. A. Howell, H. D. Enge and T. H. Kurz. 2008. “Terrestrial Laser Scanning in Geology: Data Acquisition, Processing and Accuracy Considerations.” *Journal of the Geological Society* 165 (3) (May): 625–638.

Buckley, S. J., E. Schwarz, V. Terlaky, J. A. Howell and R. W. Arnott. 2010. “Combining Aerial Photogrammetry and Terrestrial Lidar for Reservoir Analog Modeling.” *Photogrammetric Engineering & Remote Sensing* 76 (8): 953–963.

Buckley, S. J., J. Vallet, A. Braathen and W. Wheeler. 2008. “Oblique Helicopter-based Laser Scanning for Digital Terrain Modelling and Visualisation of Geological Outcrops.” *International Archives of the Photogrammetry, Remote Sensing and Spatial Information Sciences* XXXVII (Part B4): 493–498.

Burton, D., D. Dunlap, L. Wood and P. Flaig. 2011. “Lidar Intensity as a Remote Sensor of Rock Properties.” *Journal of Sedimentary Research* 81: 339–347.

Busch, H. 1991. “Ein Verfahren Zur Oberflächenmodellierung Dreidimensionaler Objekte Aus Kamerabildfolgen (Methods for Modelling of 3D Models from Image Sequences).” *Robust and Fast Modelling of 3D Natural Objects from Multiple Views*.

Butler, D. and M. Sellbom. 2002. “Barriers to Adopting Technology for Teaching and Learning.” *Educause Quarterly* (2): 22–28.

Bénitez, S. and C. Baillard. 2009. “Automated Selection of Terrestrial Images from Sequences for the Texture Mapping of 3d City Models.” In *Proceedings of the City Models, Roads and Traffic 2009 Workshop*, ed. U Stilla, F Rottensteiner, and N Paparoditis, XXXVIII:3–4.

Böhm, J. and S. Becker. 2006. “Automatic Marker-free Registration of Terrestrial Laser Scans Using Reflectance Features.” *The International Archives of the Photogrammetry, Remote Sensing and Spatial Information Sciences* 36 (5/W17): 338–344.

Dandois, J. and E. C. Ellis. 2010. “Remote Sensing of Vegetation Structure Using Computer Vision.” *Remote Sensing* 2 (4) (April 21): 1157–1176.

Debevec, P. E. and C. J. Taylor. 1996. “Modeling and Rendering Architecture from Photographs: a Hybrid Geometry- and Image-based Approach.” In *SIGGRAPH ’96 Proceedings of the 23rd Annual Conference on Computer Graphics and Interactive Techniques*, 1–10.

Duca, F., M. Cabrelles, S. Navarro, A. E. Segui, J. L. Lerma, C. Ercole and I. Este. 2011. “Photo-realistic 3D Modelling of Sculptures on Open-air Museum.” *Geoinformatics CTU FCE* 1 (2): 236–250.

Efros, A. A. and W. T. Freeman. 2001. “Image Quilting for Texture Synthesis and Transfer.” In *SIGGRAPH ’01 Proceedings of the 28th Annual Conference on Computer Graphics and Interactive Techniques*, 341–346.

Eisenbeiss, H. and M. Sauerbier. 2011. “Investigation of UAV Systems and Flight Modes for Photogrammetric Applications.” *Photogrammetric Record* 26 (136): 400–421.

El-Hakim, S. F., J. A. Beraldin, M. Picard and L. Cournoyer. 2008. “Surface Reconstruction of Large Complex Structures from Mixed Range Data – the Erechtheion Experience.” *IAPRS* XXXVII.

El-Hakim, S. F., C. Brenner and G. Roth. 1998. “A Multi-sensor Approach to Creating Accurate Virtual Environments.” *ISPRS Journal of Photogrammetry & Remote Sensing* 53: 379–391.

El-Hakim, S. F., J. Fryer, M. Picard and E. Whiting. 2004. “Digital Recording of Aboriginal Rock Art.” In *10th International Conference on Virtual Systems and Multimedia (VSMM), Ogaki City, Gifu, Japan*, 344–353.

El-Hakim, S. F, L. Gonzo, M. Picard, S. Girardi and A. Simoni. 2003. “Visualization of Frescoed Surfaces : Buonconsiglio Castle – Aquila Tower, ‘Cycle of the Months’.” *International Archives of the Photogrammetry, Remote Sensing and Spatial Information Sciences* 34 (5-W10): 1–6.

El-Hakim, S. F., M. Picard and G. Godin. 2004. “Detailed 3D Reconstruction of Heritage Sites with Large-scale Integrated Techniques.” *IEEE Computer Graphics and Applications*: 21–29.

Enge, H. D., S. J. Buckley, A. Rotevatn and J. A. Howell. 2007. “From Outcrop to Reservoir Simulation Model: Workfl Ow and Procedures.” *Geosphere* 3: 469–490.

Erikson, C. M. 2000. “Hierarchical Levels of Detail to Accelerate the Rendering of Large Static and Dynamic Polygonal Environments”. University of North Carolina.

Fabuel-Perez, I., D. Hodgetts and J. Redfern. 2009. “A New Approach for Outcrop Characterization and Geostatistical Analysis of a Low-sinuosity Fluvial-dominated Succession Using Digital Outcrop Models: Upper Triassic Oukaimeden Sandstone Formation, Central High Atlas, Morocco.” *Petroleum Geoscience* 6 (6): 795–827.

Franceschi, M., G. Teza, N. Preto, A. Pesci, A. Galgaro, and Stefano Girardi. 2009. “Discrimination Between Marls and Limestones Using Intensity Data from Terrestrial Laser Scannet.” *Journal of Photogrammetry and Remote Sensing* 64 (6): 522–528.

Frueh, C., R. Sammon and A. Zakhor. 2004. “Automated Texture Mapping of 3D City Models with Oblique Aerial Imagery.” In *Proceedings. 2nd International Symposium on 3D Data Processing, Visualization and Transmission, 3DPVT, 2004.*, 396–403.

Furukawa, Y. and J. Ponce. 2010. “Accurate, Dense, and Robust Multiview Stereopsis.” *IEEE Transactions on Pattern Analysis and Machine Intelligence* 32 (8) (August): 1362–76.

Goetz, A. F. H., G. Vane, J. E. Solomon and B. N. Rock. 1985. “Imaging Spectrometry for Earth Remote Sensing.” *Science* 228 (4704): 1147–1153.

Goldman, D.B., and J.-H. Chen. 2005. “Vignette and Exposure Calibration and Compensation.” In *Tenth IEEE International Conference on Computer Vision (ICCV’05) Volume 1*, 899–906.

Golparvar-Fard, M., J. Bohn, J. Teizer, S. Savarese and F. Peña-mora. 2011. “Automation in Construction Evaluation of Image-based Modeling and Laser Scanning Accuracy for Emerging Automated Performance Monitoring Techniques.” *Automation in Construction* 20 (8): 1143–1155.

González-Aguilera, D., J. Fernández-Hernández, J. Mancera-Taboada, P. Rodríguez-Gonzálvez and D. Hernández. 2012. “3D Modellingand Accuracy Assessment of Granite Quarry Using Unmmanned Aerial Vehicle.” *ISPRS Annals of the Photogrammetry, Remote Sensing and Spatial Information Sciences* I (3): 37–42.

González-Aguilera, D., P. Rodríguez-Gonzálvez and J. Gómez-Lahoz. 2009. “An Automatic Procedure for Co-registration of Terrestrial Laser Scanners and Digital Cameras.” *ISPRS Journal of Photogrammetry and Remote Sensing* 64: 308–316.

González-Jorge, H., D. González-Aguilera, P. Rodríguez-Gonzálvez and P. Arias. 2012. “Monitoring Biological Crusts in Civil Engineering Structures Using Intensity Data from Terrestrial Laser Scanners.” *Construction and Building Materials* 31: 119128.

Guarnieri, A., A. Vettore, F. Pirotti, M. Menenti, and M. Marani. 2009. “Retrieval of Small-relief Marsh Morphology from Terrestrial Laser Scanner, Optimal Spatial Filtering, and Laser Return Intensity. Geomorphology 113: 12–20.” *Geomorphology* (113): 12–20.

Haala, N.. 2004. “On the Refinement of Urban Models by Terrestrial Data Collection.” *International Archives of Photogrammetry, Remote Sensing and Spatial Information Sciences* 35: 564–569.

Hanusch, T. 2008. “A New Texture Mapping Algorithm for Photorealistic Reconstruction of 3d Objects.” *International Archives of Photogrammetry, Remote Sensing and Spatial Information Sciences* XXXVII (Part B5): 699–706.

Heckbert, P. S. 1986. “Survey of Texture Mapping.” *IEEE Computer Graphics and Applications* 6 (1): 56–67.

Heritage, G. and A. Large. 2009. *Laser Scanning for the Environmental Sciences*. West Sussex, UK: Wiley-Blackwell.

Hiep, V., R. Keriven, P. Labatut, L. Enpc and C. Ensam. 2009. “Towards High-resolution Large-scale Multi-view Stereo.” In *IEEE Conference on Computer Vision and Pattern Recognition, 2009. CVPR 2009.*, 1430–1437. Paris, France.

Hoppe, H. 1996. “Progressive Meshes.” In *Proceedings of the 23th International Conference on Computer Graphics and Interactive Techniques, SIGGRAPH ’96.*, 99–108.

Hoppe, H., T. DeRose, T. Duchamp, J. McDonald and W. Stuetzle. 1992. “Surface Reconstruction from Unorganized Points.” In *Proceedings of the 19th Annual Conference on Computer Graphics and Interactive Techniques - SIGGRAPH ’92*, 71–78. New York, New York, USA: ACM Press.

Horn, B. K. P. and M. J. Brooks. 1989. *Shape from Shading*. Cambridge, Massachusetts: MIT Press.

Ichokua, C. and A. Karnielia. 1996. “A Review of Mixture Modeling Techniques for Sub-pixel Land Cover Estimation.” *Remote Sensing Reviews* 13 (3-4): 161–186.

Iwaszczuk, D. and U. Stilla. 2010. “Quality Measure for Textures Extracted from Airborne IR Image Sequences.” *The International Archives of the Photogrammetry, Remote Sensing and Spatial Information Sciences* XXXVIII: 79–84.

Jones, R., K. McCaffrey, P. Clegg, R. Wilson, N. Holliman, B. Holdsworth, J. Imber and S. Waggott. 2009. “Integration of Regional to Outcrop Digital Data: 3D Visualisation of Multi-scale Geological Models.” *Computers & Geosciences* 35 (1) (January): 4–18.

Kaasalainen, S., M. Karjalainen, A. Krooks, M. Holopainen, A. Jaakkola. 2010. “Comparison of Terrestrial Laser Scanner and Synthetic Aperture Radar Data in the

Study of Forest Defoliation." *International Archives of the Photogrammetry, Remote Sensing and Spatial Information Sciences* 38 (7A): 82–87.

Khan, N. Y., B. McCane and G. Wyvill. 2011. "SIFT and SURF Performance Evaluation Against Various Image Deformations on Benchmark Dataset." In *2011 International Conference on Digital Image Computing: Techniques and Applications*, 501–506.

Klise, K. A., G. S. Weissmann, S. A. Mckenna, E. M. Nichols, J. D. Frechette, T. F. Wawrzyniec and V. C. Tidwell. 2009. "Exploring Solute Transport and Streamline Connectivity Using Lidar-based Outcrop Images and Geostatistical Representations of Heterogeneity." *Water Resources Research* 45: 1–11.

Kraus, K.. 2004. *Photogrammetry. Geometry from Images and Laser Scans*. Second edi. Berlin, Germany: Walter de Gruyter.

Kruse, F. A, R. L. Bidell, J. V Taranik, W. A. Peppin, O. Weatherbee and W. M. Calvin. 2012. "Mapping Alteration Minerals at Prospect, Outcrop, and Drill Core Scales Using Imaging Spectrometry." *International Journal of Remote Sensing* 33 (6): 1780–1898.

Kurz, T. H., S. J. Buckley, J. A. Howell and D. Schneider. 2008. "Geological Outcrop Modelling and Interpretation Using Ground Based Hyperspectral and Laser Scanning Data Fusion." *International Archives of Photogrammetry, Remote Sensing and Spatial Information Sciences* XXXVII: 1229–1234.

Kurz, T. H., S. J. Buckley, J. A. Howell and D. Schneider, 2011. "Integration of Panoramic Hyperspectral Imaging with Terrestrial Lidar Data." *The Photogrammetric Record* 26 (134) (June 6): 212–228.

Kurz, T. H., J. Dewit, S. J. Buckley, J. B. Thurmond, D. W. Hunt and R. Swennen. 2012. "Hyperspectral Image Analysis of Different Carbonate Lithologies (limestone, Karst and Hydrothermal Dolomites): The Pozalagua Quarry Case Study (Cantabria, North-west Spain)." *Sedimentology* 59 (2) (February 20): 623–645.

Lagüela, S., J. Armesto-González, P. Arias and A. Zakhor. 2012. "Automatic Procedure for the Registration of Thermographic Images with Point Clouds." *International Archives of the Photogrammetry, Remote Sensing and Spatial Information Sciences* 39 (B5): 211–216.

Lelong, C. D. 2008. "Assessment of Unmanned Aerial Vehicles Imagery for Quantitative Monitoring of Wheat Crop in Small Plots." *Sensors* 8 (5) (May): 3557–3585.

Lemmens, L. 2007. "Terrestrial Laser Scanners." *GIM International* 21: 52–55.

Lingua, A., D. Marenchino and F. Nex. 2009. "Performance Analysis of the SIFT Operator for Automatic Feature Extraction and Matching in Photogrammetric Applications." *Proceedings of the 10th CESCG Conference* 9 (5) (May): 3745–3766.

Lowe, D. 1999. "Object Recognition from Local Scale-invariant Features." In *Proceedings of the Seventh IEEE International Conference on Computer Vision*, 1150–1157.

Lubowiecka, I., P. Arias, B. Riveiro and M. Solla. 2011. “Multidisciplinary Approach to the Assessment of Historic Structures Based on the Case of a Masonry Bridge in Galicia (Spain).” *Computers and Structures* 89: 1615–1627.

Lucieer, A., S. Robinson and D. Turner. 2011. “Unmanned Aerial Vehicle (UAV) Remote Sensing for Hyperspatial Terrain Mapping of Antarctic Moss Beds Based on Structure from Motion (SfM) Point Clouds.” In *Proceeding of the 34th International Symposium on Remote Sensing of Environment, Sydney, Australia*, 1–4.

Luhmann, T., S. Robson, S. Kyle and I. Harley. 2007. *Close Range Photogrammetry: Principles, Techniques and Applications*. Wiley.

MacEachren, A. M. and J. H. Ganter. 1990. “A Pattern Identification Approach to Cartographic Visualization.” *Cartographica* 27 (2): 64–81.

Mantiuk, R., A. Tomaszewska and W. Heidrich. 2009. “Color Correction for Tone Mapping.” *Computer Graphics Forum* 28 (2) (April): 193–202.

van der Meer, F. and S. M. de Jong. 2001. *Imaging Spectrometry: Basic Principles and Prospective Applications (Remote Sensing and Digital Image Processing)*.

Meierhold, N., M. Spehr, A. Schilling, S. Gumhold, H.-G. Maas, M. Spehr and S. Gumhold. 2010. “Automatic Feature Matching Between Digital Images and 2D Representations of a 3D Laser Scanner Point Cloud.” *International Archives of Photogrammetry, Remote Sensing and Spatial Information Sciences* 38 (5): 446–451.

Nex, F. and F. Rinaudo. 2008. “Multi-image Matching: An ‘old and New’ Photogrammetric Answer to Lidar Techniques.” *IAPRS* XXXVII.

Nield, J. M., F. S. Wiggs, Giles and Robert S. Squirrell. 2011. “Aeolian Sand Strip Mobility and Protodune Development on a Drying Beach: Examining Surface Moisture and Surface Roughness Patterns Measured by Terrestrial Laser Scanning.” *Earth Surface Processes and Landforms* 36 (4): 513–522.

Niem, W. and H. Broszio. 1995. “Mapping Texture from Multiple Camera Views onto 3D–object Models for Computer Animation.” In *Proceedings of the International Workshop on Stereoscopic and Three Dimensional Imaging, Santorini, Greece.*, 99–105.

Niethammer, U., S. Rothmund, U. Schwaderer, J. Zeman and M. Joswig. 2012. “Open Source Image-processing Tools for Low-cost UAV-based Landslide Investigations.” *International Archives of the Photogrammetry, Remote Sensing and Spatial Information Sciences* 38-1/C22 (September 6): 161–166.

Nieto, J. I. and S. T. Monteiro. 2010. “3D Geological Modelling Using Laser and Hyperspectral Data.” In *Proceedings of the IGARSS 2010 Symposium*, 4568–4571.

Oppikofer, T., M. Jaboyedoff, L. Blikra, M.-H. Derron and R. Metzger. 2009. “Characterization and Monitoring of the Aknes Rockslide Using Terrestrial Laser Scanning.” *Natural Hazards and Earth System Sciences* 9: 1003–1019.

Pesci, A., G. Teza and G. Ventura. 2008. “Remote Sensing of Volcanic Terrains by Terrestrial Laser Scanner: Preliminary Reflectance and RGB Implications for Studying Vesuvius Crater (Italy).” *Annals of Geophysics* 51: 633–653.

Petsa, E., L. Grammatikopoulos, I. Kalisperakis, G. Karras and V. Pagounis. 2007. “Laser Scanning and Automatic Multi-texturing of Surface Projections.” In *CIPA International Workshop on Vision Techniques Applied, 01-06 October 2007, Athens, Greece*, 1–6.

Pierrot Deseilligny, M. and I. Clery. 2011. “APERO, an Open Source Bundle Adjustment Software for Automatic Calibration and Orientation of Set of Images.” *The International Archives of the Photogrammetry, Remote Sensing and Spatial Information Sciences* 38 (5/W16): 1–8.

Pollefeys, M., L. Van Gool, M. Vergauwen, F. Verbiest, K. Cornelis, J. Tops and R. Koch. 2004. “Visual Modelling with a Hand-held Camera.” *International Journal of Computer Vision* 59 (3): 207–232.

Portales, Cristina, Jose L. Lerma, and Carmen Perez. 2009. “Photogrammetry and Augumented Reality for Cultural Heritage Applications.” *The Photogrammetric Record* 24 (128): 316–331.

Poulin, P., M. Ouimet and M.-C. Frasson. 1998. “Interactively Modelling with Photogrammetry.” In *Eurographics Workshop on Rendering*, 93–104.

Pringle, J. K., J. A. Howell, D. Hodgetts, A. R. Westerman and D. M. Hodgson. 2006. “Virtual Outcrop Models of Petroleum Reservoir Analogues : a Review of the Current State-of-the-art.” *First Break* 24 (March): 33–42.

Püschel, H., M. Sauerbier and H. Eisenbeiss. 2008. “A 3D Model of Castle Landenberg (CH) from Combined Photogrammetric Processing of Terrestrial and UAV-based Images.” *International Archives of the Photogrammetry, Remote Sensing and Spatial Information Sciences* 37: 2–7.

Qt, 2012, http://qt-project.org/.

Remondino, F. 2006. “Image-based Modeling for Object and Human Reconstruction”. Eidgenössische Technische Hochschule (ETH), ZURICH.

Remondino, F. 2011. “Heritage Recording and 3D Modeling with Photogrammetry and 3D Scanning.” *Remote Sensing* 3 (6) (May 30): 1104–1138.

Remondino, F., L. Barazzetti, F. Nex, M. Scaioni and D. Sarazzi. 2011. “UAV Photogrammetry for Mapping and 3D Modeling – Current Status and Future Perspectives.” *International Archives of the Photogrammetry, Remote Sensing and Spatial Information Sciences* 38 (1) (September 6): 25–31.

Remondino, F. and S. F. El-Hakim. 2006. “Image-based 3d Modelling: a Review.” *Photogrammetric Record* 21 (September): 269–291.

Remondino, F., S. F. El-Hakim, A. Gruen and L. Zhang. 2008. “Turning Images into 3-D Models.” *IEEE Signal Processing Magazine* (July): 55–64.

Remondino, F. and C. Fraser. 2006. “Digital Camera Calibration Methods: Considerations and Comparisons.” *International Archives of Photogrammetry, Remote Sensing and Spatial Information Sciences* 36 (5): 266–272.

Remondino, F. and C. Ressl. 2006. “Overview and Experiences in Automated Markerless Image Orientation.” *International Archives of Photogrammetry, Remote Sensing and Spatial Information Sciences* 36: 248–254.

Remondino, F. and L. Zhang. 2006. “Surface Reconstruction Algorithms for Detailed Close-range Object Modeling.” *International Archives of Photogrammetry, Remote Sensing and Spatial Information Sciences* XXXVI: 117–123.

Riegl. 2010. “RIEGL Laser Measurement Systems.” http://www.riegl.com/.

Rittersbacher, A., S. J. Buckley, J. A. Howell, G. J. Hampson and J. Vallet. 2012. “Helicopter-based Laser Scanning: a Method for Quantitative Analysis of Large-scale Sedimentary Architecture.” *Sediment Body Geometry and Heterogeneity: Geological Society.* (Special Publications.). In Press.

Schmid, C. and A. Zisserman. 2000. “The Geometry and Matching of Lines and Curves over Multiple Views.” *International Journal on Computer Vision* 40 (3): 199–234.

Schneider, D. and H.-G. Maas. 2006. “A Geometric Model for Linear-array-based Terrestrial Panoramic Cameras.” *The Photogrammetric Record* 21 (September): 198–210.

Schneider, D. and H.-G. Maas. 2007. “Integrated Bundle Adjustment with Variance Component Estimation – Fusion of Terrestrial Laser Scanner Data, Panoramic and Central Perspective Image Data.” *International Archives of Photogrammetry, Remote Sensing and Spatial Information Sciences* XXXVI: 373–378.

Schober, A. and U. Exner. 2011. “3D Structural Modelling of an Outcrop-scale Fold Train Using Photogrammetry and GPS Mapping.” *Austrian Journal of Earth Sciences* 104 (2): 73–79.

Shirani-Mehr, M., F. Banaei-Kashani and C. Shahabi. 2009. “Efficient Viewpoint Assignment for Urban Texture Documentation.” In *Proceedings of the 17th ACM SIGSPATIAL International Conference on Advances in Geographic Information Systems, Seattle, Washington, USA*, 138–148.

Sidney, R. 2002. *Applied Photographic Optics, Third Edition*. Focal Press.

Skaloud, J., J. Vallet, K. Keller and G. Veyssiere. 2002. “HELIMAP: Rapid Large Scale Mapping Using Handheld LiDAR/CCD/GPS/INS Sensors on Helicopters.” *Natural Hazards*.

Slocum, T. A., R. B. McMaster, F. C. Kessler and H. H Howard. 2008. *Thematic Cartography and Geovisualization*. 3rd Editio. New Jersey: Pretice Hall.

Smith, M. J., A. M. Hamruni and A. Jamieson. 2009. “3-D Urban Modelling Using Airborne Oblique and Vertical Imagery.” *International Archives of the Photogrammetry, Remote Sensing and Spatial Information Sciences* 38 (7-W5): 1–6.

Snavely, N., R. Garg, S. M. Seitz and R. Szeliski. 2008. “Finding Paths Through the World’s Photos.” *ACM Transactions on Graphics* 27 (3) (August 1): 1–11.

Soudarissanane, S., R. Lindenbergh, M. Menenti and P. Teunissen. 2011. “Scanning Geometry: Influencing Factor on the Quality of Terrestrial Laser Scanning Points.” *ISPRS Journal of Photogrammetry and Remote Sensing* 66 (4) (July): 389–399.

Sturzenegger, M. and D. Stead. 2009. “Close-range Terrestrial Digital Photogrammetry and Terrestrial Laser Scanning for Discontinuity Characterization on Rock Cuts.” *Engineering Geology* 106: 163–182.

Turner, D., A. Lucieer and C. Watson. 2011. “Development of an Unmanned Aerial Vehicle (UAV) for Hyper Resolution Vineyard Mapping Based on Visible, Multispectral, and Thermal Imagery.” In *Proceeding of the 34th International Symposium on Remote Sensing of Environment, Sydney, Australia*, 1–4.

Vallet, J. 2007. “GPS/IMU and LiDAR Integration to Aerial Photogrammetry: Development and Practical Experiences with Helimap System.” In *Voträge Dreiländertagung 27. Wissenschaftlich-Technische Jahrestagung Der DGPF. 19-21 June 2007*, 1–10.

Vallet, J. and J. Skaloud. 2004. “Development and Experiences with a Fully-digital Handheld Mapping System Operated from a Helicopter.” In *The International Archives of the Photogrammetry, Remote Sensing and Spatial Information Sciences*, 3–8.

Vosselman, G. and H.-G. Maas. 2010. *Airborne and Terrestrial Laser Scanning*.

Vázquez, P. P., Miquel Feixas, Mateu Sbert and W. Heidrich. 2001. “Viewpoint Selection Using View Entropy.” In *Proceedings of Vision Modeling and Visualization Conference, Stuttgart, Germany*, 273–280.

Wang, J. and M. M. Oliveira. 2003. “A Hole-filling Strategy for Reconstruction of Smooth Surfaces in Range Images.” In *16th Brazilian Symposium on Computer Graphics and Image Processing (SIBGRAPH)*, 1–11.

Wang, R. and X. Qian. 2010. *OpenSceneGraph 3.0: Beginner’s Guide*.

Wang, Z. and C. Brenner. 2008. “Point Based Registration of Terrestrial Laser Data Using Intensity and Geometry Features.” *The International Archives of the Photogrammetry, Remote Sensing and Spatial Information Sciences* 37: 583–589.

Ware, C. 1999. *Information Visualization, Second Edition: Perception for Design (Interactive Technologies)*. Second Edi. Morgan Kaufmann.

Weinmann, M., L. Hoegner, J. Leitloff, U. Stilla, S. Hinz and B. Jutzi. 2012. “Fusing Passive and Active Sensed Images to Gain Infrared-textured 3D Models” XXXIX (September): 71–76.

Weinmann, M. and B. Jutzi. 2011. “Fully Automatic Image-based Registration of Unorganized TLS Data.” *International Archives of the Photogrammetry, Remote Sensing and Spatial Information Sciences* 38 (5/W12): 1–6.

Wessel, B., M. Huber and A. Roth. 2007. “Registration of Near Real-time SAR Images by Image-to-image Matching.” *International Archives of Photogrammetry, Remote Sensing and Spatial Information Sciences* 36 (3/W49B): 179–184.

Winkelbach, S. and F. M. Wahl. 2001. “Shape from 2D Edge Gradient.” *Lecture Notes in Computer Science* 2191 (450): 377–384.

Wolf, P. R., and B. A. Dewitt. 2000. *Elements of Photogrammetry (with Applications in GIS)*. Third Edit. New York: McGraw Hill.

Wu, C. 2012. “VisualSFM : A Visual Structure from Motion System.” http://homes.cs.washington.edu/~ccwu/vsfm/.

Wulff, R. 2010. “Image-based 3D Documentation in Archaeology.” In *32nd Annual Symposium of the German Association for Pattern Recognition*, 1–10.

Xiong, Y., K. Pulli. 2009. “Color Correction for Mobile Panorama Imaging.” In *ICIMCS ’09 Proceedings of the First International Conference on Internet Multimedia Computing and Service*, 219–226.

Zhang, Z. 1994. “Iterative Point Matching for Registration of Free-form Curves and Surfaces.” *International Journal of Computer Vision* 13 (2): 119–152.

Zhu, Q. 2010. “Multiple Close-range Image Matching Based on a Self-adaptive Triangle Constraint.” *The Photogrammetric Record* 25 (132): 437–453.